COMPARATIVE EVALUATION OF ENAMEL SURFACE ROUGHNESS AFTER MINIMALLY INVASIVE TREATMENT OF WHITE SPOT LESIONS – AN IN VITRO STUDY

I'UDZURI BIN MD JAZAM

FACULTY OF DENTISTRY
UNIVERSITY OF MALAYA
KUALA LUMPUR

2021

COMPARATIVE EVALUATION OF ENAMEL SURFACE ROUGHNESS AFTER MINIMALLY INVASIVE TREATMENT OF WHITE SPOT LESIONS – AN IN VITRO STUDY

I'UDZURI BIN MD JAZAM

RESEARCH REPORT SUBMITTED IN PARTIAL FULFILMENT OF THE REQUIREMENTS FOR THE DEGREE OF MCLINDENT IN CONSERVATIVE DENTISTRY

FACULTY OF DENTISTRY
UNIVERSITY OF MALAYA
KUALA LUMPUR

2021

UNIVERSITY OF MALAYA

ORIGINAL LITERARY WORK DECLARATION

Name of Candidate : **I'udzuri Bin Md Jazam**

Matric No : **DGI180005**

Name of Degree : **Master of Clinical Dentistry in Conservative Dentistry in Restorative Dentistry**

Title of Research Report ("this Work"): **Comparative Evaluation of Enamel Surface Roughness After Minimally Invasive Treatment of White Spot Lesions – An In Vitro Study**

Field of Study:

I do solemnly and sincerely declare that:

(1) I am the sole author/writer of this Work;
(2) This Work is original;
(3) Any use of any work in which copyright exists was done by way of fair dealing and for permitted purposes and any excerpt or extract from, or reference to or reproduction of any copyright work has been disclosed expressly and sufficiently and the title of the Work and its authorship have been acknowledged in this Work;
(4) I do not have any actual knowledge, nor do I ought reasonably to know that the making of this work constitutes an infringement of any copyright work;
(5) I hereby assign all and every right in the copyright to this Work to the University of Malaya ("UM"), who henceforth shall be owner of the copyright in this Work and that any reproduction or use in any form or by any means whatsoever is prohibited without the written consent of UM having been first had and obtained;
(6) I am fully aware that if in the course of making this Work I have infringed any copyright whether intentionally or otherwise, I may be subject to legal action or any other action as may be determined by UM.

Candidate's Signature Date: 10 March 2022

Subscribed and solemnly declared before,

Witness's Signature Date: 10 March 2022

Name:

Designation:

ABSTRACT

Objective: To investigate the surface roughness of resin infiltrated proximal white spot lesions (WSLs) with ICON® subjected to a pH cycling challenge and compare its surface roughness with WSLs treated with that of Duraphat®. **Materials and Methods:** Sixty extracted sound premolars were used in this *in vitro* study. Optical coherence tomography (OCT) was used for baseline enamel readings and randomly divided into four groups having fifteen specimens in each. Groups were assigned as: Sound (negative control), Demineralised (positive control), ICON®, and Duraphat®. All specimens except for the Sound group were subjected to an initial demineralisation in a solution containing 2.2mM calcium chloride, 2.2mM potassium meta-phosphate, and 50mM acetate buffer at a pH of 4.5 for 7 days and enamel changes were confirmed using OCT. The Sound and Demineralised groups acted as control while the other two groups were applied resin infiltration (ICON®) and fluoride varnish (Duraphat®). All the specimens were measured using a non-contact profilometer (3D Alicona) for baseline surface roughness (R_a) prior to being subjected to a pH cycling regime for 7 days. R_a analysis was after pH cycling was conducted and mean differences recorded. **Results:** Data were analysed with one-way analysis of variance (ANOVA), and repeated measure ANOVA using SPSS (ver. 23) at α=0.05. The R_a at baseline revealed significant differences across the group except for the comparison of ICON® (0.314µm±0.004) to sound enamel (0.313µm±0.028). After pH cycling the enamel surfaces treated with ICON® (0.422µm±0.004) were significantly smoother than those treated with Duraphat® (0.583µm±0.003). After 7 days of acidic challenge, ICON® exhibited the least change in R_a value (0.108µm). **Conclusions:** Within the limitations of the study, the results showed that WSLs treated with ICON® showed approximately the same surface roughness as sound enamel, suggesting suitability for the treatment of WSL.

ABSTRAK

Objektif: Untuk menkaji kekasaran permukaan lesi bintik putih proksimal (WSL) yang diinfiltrasi dengan ICON® dibawah cabaran kitaran pH dan membandingkan kekasaran permukaannya dengan lesi bintik putih proksimal yang dirawat dengan Duraphat®. **Kaedah:** Enam puluh gigi geraham kecil yang telah diekstraksi telah digunakan dalam kajian *in vitro* ini. Tomografi koheren optik (OCT) digunakan untuk bacaan imbasan asas enamel dan dibahagikan secara rawak kepada empat kumpulan yang masing-masing mempunyai lima belas spesimen. Kumpulan dikategorikan sebagai: Sihat (kawalan negatif), Demineralisasi (kawalan positif), ICON®, dan Duraphat®. Semua spesimen kecuali kumpulan Sihat mengalami demineralisasi awal dalam larutan yang mengandungi 2.2mM kalsium klorida, 2.2mM kalium meta-fosfat, dan 50mM asetat sebagai penyangga pada pH 4.5 selama 7 hari dan perubahan pada enamel disahkan menggunakan OCT. Kumpulan Sihat and Demineralisasi bertindak sebagai kumpulan kawalan sementara dua kumpulan yang lain menggunakan infiltrasi resin (ICON®) dan varnis fluorida (Duraphat®). Semua spesimen dianalisa menggunakan profilometer tanpa sentuhan (3D Alicona) untuk bacaan kekasaran permukaan asas (R_a) sebelum menjalani rejim kitaran pH selama 7 hari. Analisis R_a dilakukan setelah kitaran pH dilakukan dan perbezaan min dicatatkan. **Keputusan:** Data dianalisis dengan menggunakan one-way ANOVA, dan repeated-measure ANOVA. Semua analisis dilakukan menggunakan program SPSS versi 23 (USA). Perbezaan dengan nilai P <0,05 dianggap signifikan secara statistik. R_a pada awal menunjukkan perbezaan yang ketara pada seluruh kumpulan kecuali untuk perbandingan ICON® (0,314µm ± 0,004) dengan enamel sihat (0,313µm ± 0,028). Setelah kitaran pH dilakukan, permukaan enamel yang dirawat dengan ICON® (0,422µm ± 0,004) lebih licin berbanding yang dirawat dengan Duraphat® (0,583µm ± 0,003). Setelah 7 hari melalui cabaran berasid, ICON® menunjukkan perubahan nilai kekasaran R_a paling sedikit (0.108µm). **Kesimpulan:** Dalam batasan kajian, hasil

menunjukkan bahawa WSL yang dirawat dengan ICON® menunjukkan kekasaran permukaan yang hampir sama dengan enamel sihat, menunjukkan kesesuaian untuk digunakan untuk rawatan WSL.

ACKNOWLEDGEMENTS

Bismillahirramanirrahim, in the name of ALLAH, the most gracious and most merciful. Alhamdulillah, the highest gratitude and praise to ALLAH the Almighty, only with His blessings and grace, I am to complete this research report on "Comparative Evaluation of Enamel Surface Roughness After Minimally Invasive Treatment of White Spot Lesions – An *In Vitro* Study". There are many people who have guided, supported and helped in completing this research. Therefore, I would like give the greatest of gratitude and acknowledgement to those who had made this possible for me and for everything else. Special and thousands of appeciations to:

1. Dr Angela Maria Garcia Gonzalez, who has patiently guided and supported me throughout the completion of this research.
2. Associate Professor Dr Prema Sukumaran, for all the endless support, ideas, advice given and also trust and freedom of decision making during this journey.
3. Associate Professor Dr Azwatee Abd Aziz, for all her insightful comments, immense knowledge, and motivations.

   I truly believe all three have been immense in making this journey possible. I could not have imagined having better advisors and mentors for my research.
4. All the staff in the Biomaterial Research Lab (BRL) especially Madam Helen and Madam Zarina in helping to facilitate my work in many ways. I am truly grateful.
5. My colleagues, who have been great companions and help during our time as postgraduate students.
6. To my mother (mama) and father (ayah) who I owe everything in life for. No words could express my gratitude for all the selfless and ceaseless support they have given me throughout life. Mama, you're the strongest women I know. We will make it through this together. I promise.

7. My sisters, for all the supports and love you've given. I know we will always have each other's back.
8. My in laws, in this truly testing time, have always been there for me and my family.
9. My wife Atiqa and son Harris for their devoted love, support and understanding. I could never thank you enough for being the pillars of my strength. I love you both endlessly.

I am forever grateful to those I have identified, and others not mentioned here, who have helped directly or indirectly in the making of this research. May Allah bless all of you.

"One can pay back the loan of gold, but one dies forever in debt to those who are kind"

TABLE OF CONTENTS

LIST OF FIGURES

LIST OF TABLES

LIST OF SYMBOLS AND ABBREVIATIONS

2D	:	Two-dimensional
3D	:	Three-dimensional
AFM	:	Atomic force microscope
ANOVA	:	Analysis of variance
Ca	:	Calcium
$Ca_{10}(PO_4)_6(OH)_2$	:	Hydroxyapatite
$Ca_{10}(PO_4)_6Cl_2$	:	Chlorapatite
$Ca_{10}(PO_4)_6F_2$	:	Fluorapatite
CPP-ACP	:	Casein phospho-peptide amorphous calcium phosphate
CF	:	Contact facet
Cl	:	Chloride
CLSM	:	Confocal laser scanning microscopy
CT	:	Computed tomography
Cu	:	Copper
DEJ	:	Dentino-enamel junction
F	:	Fluorine
FAp	:	Fluorapatite
FD	:	Fourier domain
Fe	:	Iron
FWHM	:	Full width half maximum
H_3PO_4	:	Phosphoric acid
HAp	:	Hydroxyapatite
HCL	:	Hydrochloric acid
HEMA	:	2-hydroxyethyl methacrylate

ICDAS	:	International caries detection and assessment system
ICON®	:	Infiltration concept
IR	:	Infrared
K	:	Potassium
KCl	:	Potassium chloride
LED	:	Light emitting diode
MID	:	Minimally invasive dentistry
MR	:	Magnetic resonance
OH	:	Hydroxyl
pH	:	Potential hydrogen
PC	:	Penetration coefficient
PO_4	:	Phosphate
PS-OCT	:	Polarisation-sensitive optical coherence tomography
PVS	:	Polyvinyl siloxane
Ra	:	Radium
RI	:	Refractive index
SD	:	Standard deviation
SEM	:	Scanning electron microscopy
Sr	:	Strontium
SS-OCT	:	Swept-source optical coherence tomography
TEGDMA	:	Triethylene-glycol-dimethacrylate
TM	:	Transverse microradiography
WSL	:	White spot lesion
Zn	:	Zinc

LIST OF APPENDICES

CHAPTER 1: INTRODUCTION

1.1 Background and Research Problem

Dental caries is one of the most common chronic oral diseases found not only in Malaysia but also worldwide (G. S. Kumar, 2015). The contemporary definition of dental caries is as follows: "*caries is a dynamic, complex, multifactorial process involving the gradual loss of mineral compounds from hard dental tissue*" (Kidd et al., 2016). The current understanding is that dental caries is a slow progressing disease which involves local factors such as the formation of microbial biofilm and diet based on fermentable carbohydrates. It can further be influenced by modifying factors such as the frequency of oral hygiene and the individual's social status (Roberson et al., 2006). The formation of caries occurs due to the demineralisation of enamel mainly caused by lactic acids produced by cariogenic bacteria such as Streptococcus mutans and Scardovia wiggsiae (Featherstone, 2008; Mann et al., 2006). If the biofilm's pH level falls below the critical level (5.5) and is not removed, minerals such as hydroxyapatite are loss which in turn causes an increase in the porosity between the enamel crystals. This softens the surface and allows the diffusion of acids into the tooth resulting in demineralisation of the enamel subsurface. The increase in microporosities causes the appearance of a white spot on the enamel (Mann et al., 2006; Roberson et al., 2006).

White spot lesions (WSLs) therefore represent the initial demineralisation of the enamel. A rough and white-opaque appearance can be observed when in an active state but exhibits a shiny and smooth surface when it is inactive (Kidd et al., 2016). WSLs on occasions can be seen as a brown colouration due to the absorption of extrinsic pigments by decalcified enamel (Groeneveld et al., 1990; Park et al., 2011). According to the International Caries Detection and Assessment System (ICDAS), the WSLs with no

evidence of surface breakdown or underlying dentine shadowing can be scored a 1 (initial caries) or 2 (distinct visual change in the enamel) (Banting et al., 2005).

In terms of tooth surface cavitation, the proximal areas are more susceptible and have a higher risk of being carious (Larsen et al., 1989). Proximal areas have a high prevalence due to their difficulty in cleaning the areas coupled with poor dental hygiene compliance of patients. In the past, invasive treatment methods of drilling and filling which required the removal of marginal tissue weakened the residual tooth structure (Larsen et al., 1987). Further understanding of caries development coupled with advancements in technologies has seen a change in paradigm where non-invasive or microinvasive treatments are favoured over traditional restorative methods. The contemporary protocols aim to restore the tooth structure in a manner that is both cost friendly and painless and in tandem is able to regain function and aesthetics (Cury et al., 2009; Harris et al., 2004; Silverstone, 1982; Ten Cate, 2003).

Non-invasive treatments manage caries lesions via mechanical removal of the biofilm, dietary control or remineralisation treatments (Bader et al., 2001). Toothbrushing and interdental flossing, together with good dietary control, focus on prevention rather than halting carious lesion progression (Bader et al., 2001; Gomez, 2015). Remineralisation of the enamel lesion with fluoride or casein phosphopeptide amorphous calcium phosphate (CPP-ACP) is promising (Karlsson, 2010; Silverstone, 1982), and often recommended as the treatment of choice for initial enamel caries on smooth or proximal surfaces, but its effectiveness is highly dependent on patient's oral hygiene practices and is contraindicated in noncompliant patients (Peters et al., 2001; Silverstone, 1982). Consequently, micro-invasive treatments have been developed as alternatives since they are less dependent upon patient compliance and are still more conservative than other invasive treatments. This alternative therapy arrests initial caries lesions by infiltrating

microporosities within the enamel lesions using a low-viscosity liquid resin (Adriaenssens et al., 2017; Dorri et al., 2015; Machoy et al., 2017).

Micro-invasive treatments are applied to manage the lesions confined to the outer third of dentine and involve the preliminary treatment of the tooth surface using a conditioning step via organic acid where only micrometres of the enamel layer are removed (Drexler et al., 2008; Feldchtein et al., 1998). This will keep the surface of the carious lesions intact and preserved. Infiltration and sealing are frequently used as options in microinvasive treatments. Recently, infiltration technology has been performed clinically for non-cavitated proximal caries (Arnaud et al., 2010; Braz et al., 2011). Based on capillary forces, the low viscosity resin penetrates the pores of demineralised enamel and upon setting establishes a barrier impeding acid diffusion (Hariri et al., 2012; Ishibashi et al., 2011; Senawongse et al., 2011). The appearance of white spots on the enamel is a result from the optical effect of light scattering, which occurs due to different refractive indexes (RIs). When the porosities on the enamel are filled with air (RI 1.00), a greater light dispersion will occur. This is due to lower RIs of the hydroxyapatite (1.62 to 1.65), leading to an opaque and whitish appearance (Potsaid et al., 2010). White spot may remain even when fluoride treatment is performed. This happens because remineralisation occurs only superficially. In contrast to the infiltration technique, the interior of the lesion or enamel subsurface is filled with resin by capillary action. Since the RI of the resin (1.51) is similar to that of the hydroxyapatite, masking of the lesion is also possible (Colston et al., 1998; Fried et al., 1995; Otis et al., 2000; Potsaid et al., 2010; Wilder-Smith et al., 2008; Yun et al., 2003). Previous systematic reviews and meta-analyses have shown that micro-invasive treatments are more effective than non-invasive treatments (Arnaud et al., 2010; Drexler et al., 2008; Holtzman et al., 2010; Jang, 2014; Lakshmikantha et al., 2017; Larsen et al., 1987).

Fluoride varnish when painted on to enamel hardens to a clear or slightly yellowish film. The mechanism of action is by release of fluoride ion to the underlying tooth surface. The availability of fluoride in the liquid phase around the apatite crystallites blocks crystalline dissolution and reduces the rate of demineralization. Increased fluoride ion activity that results after fluoride varnish treatment in sound or carious enamel, actually enhances mineral deposition and promotes remineralisation (Rølla et al., 1993).

In normal physiological conditions, the surfaces of teeth are in a state of constant, alternating periods of demineralisation and remineralisation. At the initial stage, the course of the disease is dynamic (Roberson et al., 2006). Prophylaxis and treatment using minimally invasive methods influences the rate of demineralisation and remineralisation. When remineralisation exceeds the rate of demineralisation, the caries may stop developing or even heal, which results in a smoother surface (Huysmans et al., 2004; Kidd et al., 2016; Kim et al., 2011). On the other hand, when more demineralisations happen, it leads to an increase in the porosity and roughness of the enamel. Rough surfaces are retention sites for plaque and risk factors for secondary caries development. Furthermore, rough surfaces are vulnerable to staining from coffee, tea or red wine and become darker over time. In bovine enamel, resin infiltration into the enamel surface has been shown to primarily result in a smoothening of the surface (El Karim et al., 2007).

Testing enamel surface roughness is a useful means of assessing the activity and stage of a carious lesion and plays a significant role in the colonisation and retention of bacteria. Smoothing out the enamel surface can thus play an important role in preventing this disease (Schlüter et al., 2011). In addition, a perfectly smooth surface ensures a shine, which improves the overall visual acceptance of the colour of a tooth.

Caries infiltration is considered a micro-invasive treatment option for non-cavitated enamel lesions extending to the outer third of dentine (Featherstone et al., 1983). ICON®

(DMG Chemisch-Pharmazeutische Fabrik GmbH, Hamburg, Germany) is a commercially available resin infiltrant material developed to arrest intermediary lesions in one visit with no mechanical preparation or anaesthesia. It has been proposed that the theory of tooth surfaces being intact adjacent to carious lesions, especially interproximal lesions, is false and that these surfaces are, in fact, not intact (Kielbassa et al., 1999). The approximal version of the product is specially developed for hard tissues, preserving treatment of incipient proximal caries. Not much is known about the long-term stability of the resin and the possible effects of the surface alterations. Resin degradation might result in surface destruction and the development of plaque on these sites due to increase in surface roughness (Lussi, 2006). Therefore, resin degradation may be a risk factor for increased plaque accumulation and the development of secondary caries.

As noted above, the problem currently with the existing *in vitro* clinical validation of anti-caries modalities for preventing caries is due to the non-availability of studies that considered the method of delivery of the materials that simulated an *in vivo* condition. Furthermore, most published surface roughness data for enamel has been measured on ground sections, while only several on intact enamel surfaces. No other studies simulated the application of materials to the dentition with intact proximal contacts.

This research evaluated the difference in surface roughness of white spot lesion treated with resin infiltrant and fluoride. In our research, the methodology incorporated by applying the materials using a customised jig to simulate the intraoral conditions was the novelty of the study. With this, it is hoped that it will serve as a standard for any future studies. The importance of eliminating any inevitable variability of *in vitro* studies especially in proximal surface roughness evaluation would therefore be a significant contribution to the scientific and clinical research community.

1.2 Research Purpose and Questions

In view of the research problem discussed above, the purpose of the study was to determine whether treatment of white spot lesions using minimally invasive techniques could prevent further colonisation and retention of bacteria by maintaining a surface roughness within the maximum threshold.

This research purpose was guided by the following research questions,

1. Will the use of a resin infiltrant and fluoride varnish on a WSLs exhibit the same surface roughness?
2. Will the effect of pH cycling change the surface roughness of WSLs treated with resin infiltrant and fluoride varnish?

1.3 Research Hypothesis

There is statistically significant difference between the surface roughness of artificial proximal WSLs treated with resin infiltrant and fluoride before and after pH cycling.

1.4 Aims and Objectives

To investigate and compare surface roughness of proximal white spot lesions (WSLs) treated with ICON® and Duraphat® after placement and after 7 days of acidic challenge.

In order to achieve this aim, the research objectives were as follows:

1. To determine and compare surface roughness of proximal WSL treated with resin infiltrant and fluoride.
2. To compare changes in the surface roughness of enamel treated with resin infiltrant and fluoride after pH cycling.

1.5 Null Hypothesis

There is no statistically significant difference between the surface roughness of artificial proximal WSLs treated with resin infiltrant and fluoride before and after pH cycling.

CHAPTER 2: LITERATURE REVIEW

2.1 Introduction

This chapter begins with discussions on the structure of the tooth, specifically the enamel which is a complex structure and the understanding of the pathophysiology of early approximal caries relies on the knowledge of its structure. Generally, enamel demineralisation can be seen in the form of dental fluorosis, opacity and white spot lesions. White spot lesions (WSLs), occur as a result of subsurface enamel demineralisation with detection and treatment of these early approximal caries proving vital in preventing the progression of the lesion. Different caries detection tools have been developed and their suitability will be discussed and evaluated. Therapeutic and preventive techniques such as resin infiltrations and fluoride application for early approximal caries arrest have been developed and introduced for management will be reviewed.

2.2 Structure of the Tooth

2.2.1 Enamel

2.2.1.1 Physical Characteristics of Enamel

Enamel is calcified tissue and forms the outer-most layer of the tooth coronal structure forming a protective covering of variable thickness (G. S. Kumar, 2015). It is able to attain a maximum thickness of about 2 to 2.5 mm on the cusps of the human molars as well as the premolars, thinning down to almost a blade-like edge at the cervical aspects of the tooth. The basic units of enamel comprise of the enamel rods, rod sheaths and interprismatic substances. The cells responsible for enamel formation are the ameloblasts. When the tooth completes its formation, these ameloblasts undergo a programmed cell death called apoptosis and are lost and hence enamel is unable to regenerate itself. Due

to this inherent limitation, enamel becomes a noncellular and nonvital tissue (Akasapu et al., 2018).

Enamel is the hardest calcified tissue in the body due to its high mineral content and highly ordered crystalline molecular arrangement (G. S. Kumar, 2015). The main function of enamel is to form a resistant covering of the tooth structure, rendering it suitable for mastication. Its structure and hardness render it brittle, as is apparent when it loses dentine support.

The colour tones of the tooth vary from yellowish white to greyish white, which is established by the translucency of enamel and underlying dentine. Greyish teeth have thick opaque enamel while the yellow-tinged teeth have thin translucent enamel, as a result of reflections from the yellowish coloured dentinal layer. The degree of calcification of the enamel structure and its homogeneity that influences this translucency (G. S. Kumar, 2015). In caries lesions, changes in colour of the enamel specifically are attributed to changes in its refractive index (RI) as a result of porosities in the subsurface layers of enamel (Kidd et al., 2016).

2.2.1.2 Chemical Properties of the Enamel

Enamel is made up of 96% similar to apatite inorganic components and the remaining 4% comprises of organic material and water. The largest mineral constituent present as a crystalline lattice framework is the calcium-deficient carbonate-containing apatite making up about 92% of the mineral content by volume (Roberson et al., 2006). Other minerals are Na, Cl, K, and F; Zn, Fe, Sr, Ra, and Cu are found in trace amounts. The main components of the apatite family are hydroxyapatite (OHAp, $Ca_{10}(PO_4)_6(OH)_2$), chlorapatite (ClAp, $Ca_{10}(PO_4)_6Cl_2$), carbonated apatites and fluorapatite (FAp, $Ca_{10}(PO_4)_6F_2$) (Leroy et al., 2001).

2.2.1.3 Structure of the Enamel

Enamel's primary structural component comprises of millions of enamel rods and prisms, as well as the rod sheaths and a cementing inter-rod element in some of its areas (G. S. Kumar, 2015). It is estimated that the number of enamel rods can be as many as 5 million in lower incisors to 12 million in the upper first molar. The rods run from the dentino-enamel junction towards the enamel surface of the tooth. The span of the rods is greater than the thickness of the enamel, because of the wavy and oblique direction of the rods. In the cusps, the thickest part of the enamel, the rods are longer compared to those in the cervical area of the tooth. According to De Menezes Oliveira et al., the mean diameter of the rods varies from approximately 3.84 μm from where it originates at the enamel dentinal junction to 4.34 μm on the outer surface of the enamel (De Menezes Oliveira et al., 2010). They appear to be hexagonal with clear crystalline appearance, allowing light to pass through them. Sometimes when viewed in cross-section under the light microscope, they appear round or oval in shape (G. S. Kumar, 2015).

2.3 Pathophysiology of Caries

2.3.1 Enamel Changes During Early Approximal Caries Lesion Development

Dental caries has been referred to as an infectious microbiologic disease of the teeth that leads to localised dissolution and destruction of calcified tissues (Roberson et al., 2006). There is a multiplicity of factors which influence caries formation. These factors are bacterial plaque, fermentable carbohydrates, susceptible surfaces of tooth, and time.

The process which triggers demineralisation and dissolution of tooth structure comes from a localised drop in the pH at the plaque-tooth interface. The local pH drop takes place due to high bacterial concentrations of *Mutans Streptococci* and *Lactobacillus* responsible for producing acids which cause the drop in pH of the saliva partly triggering the tooth demineralisation process. Bacteria are able to live in a range of ecological niches

and prime examples of such niches are the occlusal fissures and the approximal spaces between neighbouring teeth.

Exposure to sucrose and unsatisfactory oral cleanliness aid bacterial colonisation, which in-turn metabolises fermentable carbohydrates to produce organic acids. These bacterial by-products readily diffuse in all directions including into the pores of enamel and dentine. Soluble minerals such as calcium and phosphate are attacked by the acid, they are dissolved into the surrounding aqueous phases between the crystal lattices. Roughly around 1 in 10 in enamel, and 1 in 5 in dentine phosphate ions are replaced by carbonate ions. This process creates defects and calcium deficient regions (Featherstone, 2008).

Having said that, a change to the mineral contents on the surface of the tooth is not dependant on this single event, rather many more episodes are needed over a longer time frame to produce this cariogenic effect. When the pH falls to a value of about 5.5, the acidity from the caries-active plaque overcomes the buffering capacity of salivary bicarbonate resulting in the dissolution of tooth surface minerals and loss of its calcium and phosphate ions (Roberson et al., 2006).

At pH values of 4.0 or lower, the intact enamel is etched and roughened while undergoing subsurface mineral loss. In other words, this initial enamel disintegration process is characterized by an intact enamel surface with subsurface demineralisation (Roberson et al., 2006). The clinical chalky white appearance of this incipient lesion is resultant from the subsurface porosity and not detectable when hydrated. The drying of this lesion with air removes the subsurface water, leaving air-filled voids, and due to different refractive indexes, making the area appears opaque and white. These incipient lesions can be reversed with the process of remineralisation. When the subsurface demineralisation is so extensive, the enamel structure collapses, and cavitation happens.

This substantial structure loss is not reversible and is associated with the destruction of the tooth structure (Roberson et al., 2006).

A multistep process involving bacteria, diet and host factors forms a triad involved in the formation of a carious lesion. Susceptibility to demineralisation is due to enamel's high mineral content. This occurs for several reasons, but the most evident cause is the ingestion of sugars. A variety of intraoral bacteria interacts with carbohydrates and as a result from fermentation, it produces organic acid such as lactic, formic, acetic and pyruvic acids which decreases the pH in the mouth. Some tooth morphologies can be deemed impossible for cleaning using toothbrushes and other oral cleaning instruments that affect the cleaning efficacy and thus further dictate bacterial adhesion. The amount of sugar does not contribute to tooth decay, but the frequency of sugar ingestion leaves the enamel vulnerable to acid attacks. These acids act on the hydroxyapatite crystals frees calcium and phosphate minerals initiating the process of cavity formation. Remineralisation of the lesion is possible not only as a result of intraoral pH fluctuations but also by the activity of ionic motion and consequent dissolution and destruction of apatite crystals. The absorption of fluoride ions can substitute the acidic OH radicals, forming fluorapatite, a more stable and resistant to acid attack crystal, and this is why the applications of fluorides can help in remineralisation and caries prevention (Kaitsas et al., 2015).

2.3.2 Approximal White Spot Lesion

The earliest signs of a carious lesion on a tooth surface that can be spotted with an unaided eye is often referred to as white spot lesion (WSL). Other terms used in literatures and studies are initial, early or incipient lesions. These terms are implied to describe the initiatory state or earliest stages of lesion development (Machale et al., 2013). Nonetheless, inaccuracies in using the terms may arise as a WSL may have been present

for many years in its arrested state before being noticed. The definition of "incipient" is "beginning; an initial stage". To put it simply, an initial detectable lesion appears as a chalky white, opaque change (a white spot), however, those WSLs are not incipient (Kidd et al., 2016). The kidney-like appearance of the WSL between the contact facet and gingival margin is determined by the distribution of microbial deposits. Clinically seen on the approximal surfaces are facet areas partly surrounded by cervically directed opaque areas. Interestingly, the shape of the gingival margin forms the cervical border of the lesion. The active and inactive lesions can be reflected in accordance with host efforts to clean and control plaque accumulations. It is possible to see the opaque areas extends into the buccal and lingual directions (Figure 2.1) parallel to the gingival margin as a result of neglected oral hygiene (Mann et al., 2006).

Figure 2.1 Plaque accumulations and formations of WSL in posterior teeth. (A) showing tooth that are in contact. (B) the tooth premolar is removed for better visualisation showing plaque accumulations on the approximal and buccal cervical surfaces that are part of a continuous ring of plaque around the tooth. WSL visible just below the tooth contact area results in a kidney-shaped appearance. (C) WSL is able to extend buccally and lingually in cases of neglected oral hygiene.

When analysing the surface of an active WSL through the scanning electron microscope, distinct changes can be seen on approximal surfaces at a magnification as low as 50x (Akasapu et al., 2018). The contact aspect of the approximal surface has a smooth look where the perikymata has been abraded, however irregular fissures and other

small defects can be seen along the periphery of the facet (Figure 2.2). The enamel surface cervical to the facet has deepened and more irregular Tomes' processes pits when in close vicinity appear to merge together, forming larger irregular porosities, cracks or fissures.

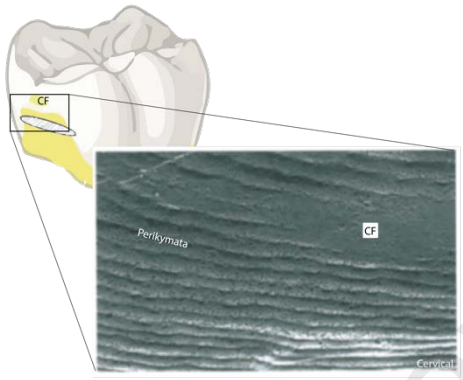

Figure 2.2 A close look at the surface of approximal white lesion by using scanning electron micrograph. The insert (adapted from Essentials of Dental Caries, 3rd Edition) displays early surface abrasion to the contact aspect or facet (CF) and surface irregularities cervical to it.

Tomes' processes are histological projections which is located on the secretory, basal end of ameloblasts. A fully developed Tomes' process is a distal extension or a projection of the ameloblasts consisting of a proximal and distal portion. It forms and interdigitates with the enamel as the ameloblast moves away giving a "picket-fence" or "saw-tooth" appearance. Enamel matrix proteins are secreted through the Tomes' process and orchestrate the mineralisation process that produces apatite fibres and their alignment. Rod and interrod enamel are a result of a Tomes' process. 'Pits' formation is a consequence of an asymmetric deposition of matrix protein which happens at 2 secretory sites: the proximal and distal portion of the Tomes' process. Enamel matrix secreted by the proximal portion surrounds the enamel matrix secreted by the distal portion. This distal portion enamel matrix forms the enamel rods while the enamel matrix from the proximal Tomes' process that surrounds the rod forms the interrod enamel. As the matrix continues to be secreted, the distal portion of Tomes' process does not only elongate, but also becomes thinner and gradually dissipates leaving a thin space between the rod and

interrod that is filled with organic materials to form the enamel sheath. As the ameloblast undergoes apoptosis, the final layer of enamel matures and does not contain any rod. In early phases of enamel dissolution, the rods are exposed and disintegration leading to microcavities of the enamel surfaces happens (Figure 2.3) (Warreth et al., 2020).

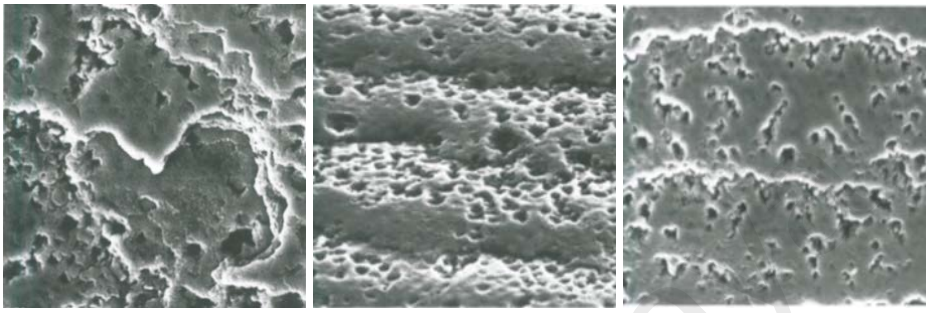

A B C

Figure 2.3 A detailed look at the surface dissolution patterns. Cervical to the contact facet, uncountable irregularities in the opaque surface are seen resultant from deepened and more irregular Tomes' processes pits and increased number of eroded focal holes. (A, B, C) when this pits and holes merge together and forms larger areas of defects (adapted from Essentials of Dental Caries, 3rd Edition)

2.3.3 Demineralisation and Remineralisation of the Enamel

2.3.3.1 Demineralisation

Enamel is vulnerable to an acidic environment. When the pH of saliva or plaque decreases, the solubility of the hydroxyapatite increases dramatically. Approximately, the solubility of hydroxyapatite is boosted by a factor of 10 with a drop of each single pH unit (Groeneveld et al., 1990). The acidic environment leads to two distinct types of lesions: caries lesion and erosion. The initial stages of carious lesion formation are defined by partial dissolution of the enamel surface, almost an erosion-like reaction, but once the acidic reactions are reversed, the process instantaneously results in a 20 - 50 μm thick, mineralised enamel surface layer with mineral loss of the subsurface body of the lesion. As these processes continue over extended periods of time, approximately 30 - 50% mineral loss occurs, extending deep into the enamel and dentine, at the same time

leaving a 20 - 80 μm thick, rather well mineralized surface area intact (Park et al., 2011). The differences in histological features of a caries lesion and erosion are reflected in their clinical appearance: the former is chalky white and porous, while the latter appearance of eroded enamel is usually hard and shiny.

As the hydrogen ion concentration is lowered in the oral fluids, resulting in a reduction in the concentration of hydroxyapatite and at a critical pH of 5.5 (Schmidt-Nielsen, 1946), the oral fluids become saturated with hydroxyapatite. Bear in mind, this critical pH is not constant. It is a person-specific parameter and can be more dynamic depending on other factors such as diet and plaque formation. The solubility of fluorapatite is less than hydroxyapatite. Plaque fluid remains supersaturated with fluorapatite and undersaturated with respect to hydroxyapatite (Figure 2.4 and Figure 2.5). Fluorapatite also has a critical pH estimated to be in the region of 4.5, which is one unit lower than for hydroxyapatite. Like hydroxyapatite, the critical pH varies in different individuals. As the subsurface hydroxyapatite is dissolved, fluorhydroxyapatite is formed on the outermost surface layers of the enamel.

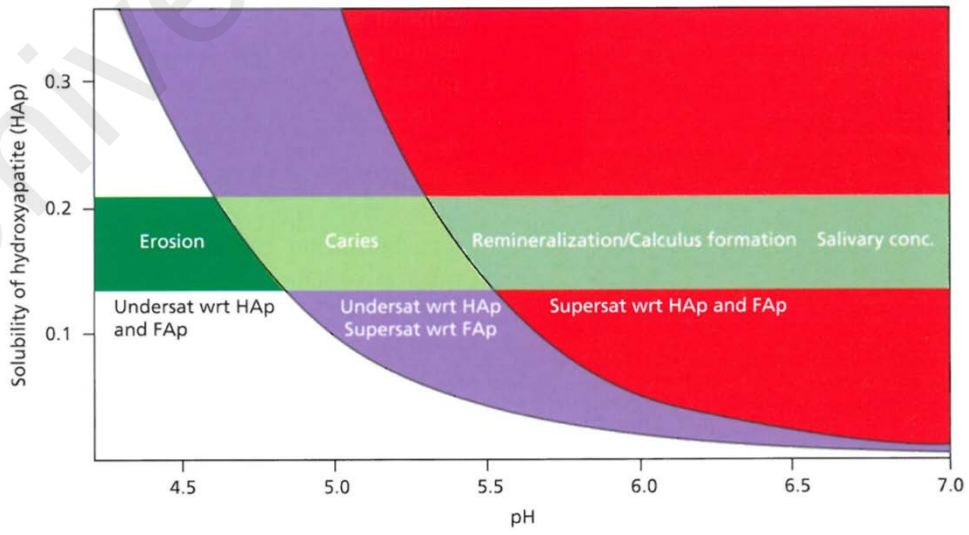

Figure 2.4 Solubility of hydroxyapatite (HAp) and fluorapatite (FAp) as a function of pH in the range 4 – 7. In saliva, a caries lesion may develop in the condition where there is an increased dissolution of HAp, causing supersaturation of FAp. (adapted from Essentials of Dental Caries, 3rd Edition)

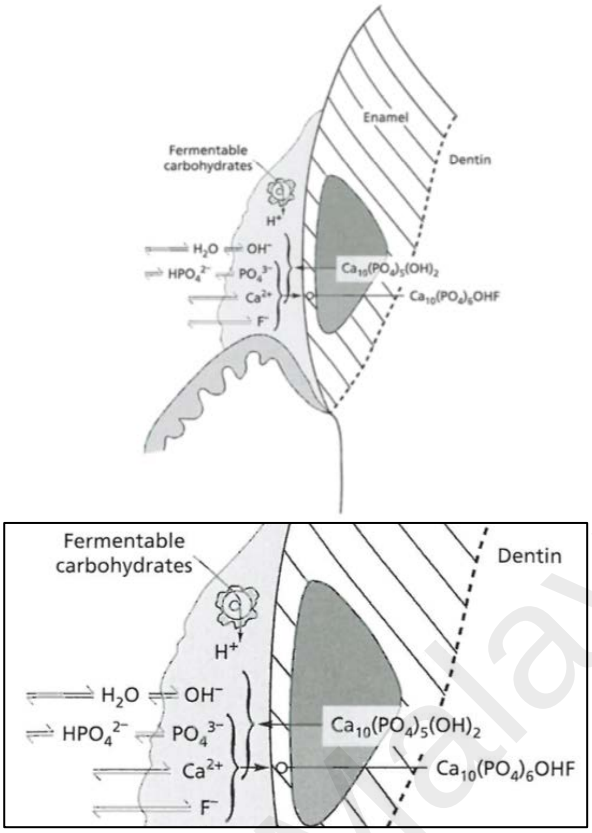

Figure 2.5 A schematic drawing showing the effect of the numerous pH fluctuations in the biofilm on the dental enamel. This diagram reflects the solubility of hydroxyapatite and fluorapatite as a function of pH in the range of 4.5-5.5 as demonstrated in Figure 2.4. While hydroxyapatite dissolves in the subsurface region the fluoridated apatite can build up in the surface layer of the tooth. (Field et al., 2010)

Maintenance and integrity of the enamel surface is due to the concurrent supersaturation of fluorapatite. To put it into perspective, the more supersaturated the solution, in regard to fluorapatite, the thicker and less demineralised the layer remains (Park et al., 2011). Nevertheless, it is essential to appreciate that in a countless pH fluctuating cariogenic oral environment, these surface zones will undergo constant surface dissolution with mineral redepositing indefinitely, which in turn can be shown by the irregular, moth-eaten-like surface appearance, as seen through microradiography (Figure 2.6). This build-up of fluorapatite leads in time to a high content of fluorhydroxyapatite at the expense of hydroxyapatite in the surface layer of the carious lesion. It must be noted that as long as the surface layer remains intact with reasonable

mineral contents, there will be absence of fluoride diffusion into the lesion hence reflected in the idle fluoride concentration in the subsurface body of the lesion. Rather, fluoride responds by diffusing inwards causing predominantly fluorhydroxyapatite formation in the outer layers. If fluctuations of the pH are in the range of 4.0 – 5.6, a protective effect is triggered which is exerted by the surface layer preventing further dissolution (Kidd et al., 2016).

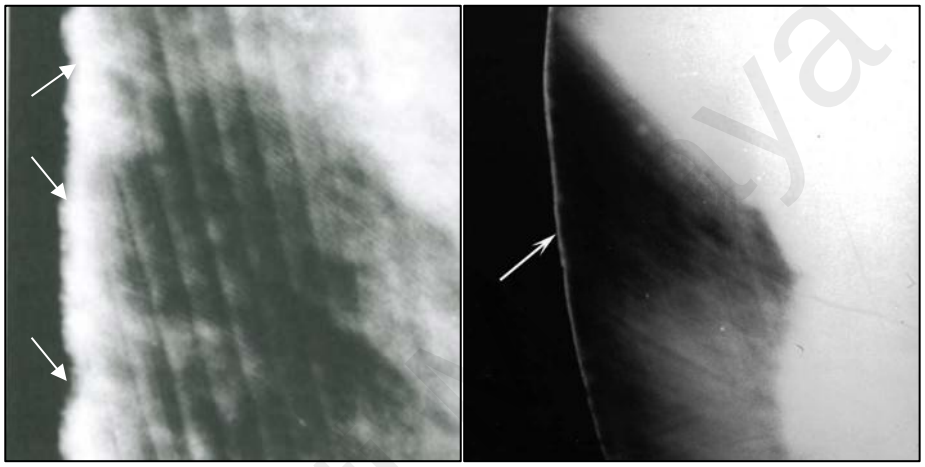

A B

Figure 2.6 Examples of microradiogram depicting varying loss of mineral in the body of the lesion. (A) Visible cross striation of several prisms in the body of the lesion with moth-eaten like appearance on the tooth surface. (B) A moth-eaten appearance on a well mineralised inactive enamel surface layer.

2.3.3.2 Remineralisation

A single pH fluctuation in the plaque is highly unlikely to impact the formation or regression of caries. The rate of dissolution as mentioned in the demineralisation section, depends not only pH, but other factors as well. When the surface disintegrates, a larger effect of the pH will be exerted on the subsurface. Saliva is rich in calcium and phosphate ions. It acts as a buffer to neutralise the acidic environment. The reversal of demineralisation can be achieved at pH of >5.5 together with high concentration of calcium and phosphate. It is imperative to remember, concentration of calcium and phosphate varies in individuals which in part may explain the susceptibility to caries

during childhood due to their lower saliva calcium concentrations. In this process calcium phosphates reprecipitates and the region of demineralisation is remineralised.

There are a few extreme laboratory experiments (Larsen et al., 1987, 1989) conducting research in attempts to fill the pores of demineralised enamel lesions with phosphate and calcium ions with pH above the critical limits and compared their observations with *in vivo* natural conditions. Their observations did not tally with the *in vivo* situations in the sense that no remineralisation occurred within caries but instead are formed and restricted to the tooth surface. They concluded remineralisation of dental lesions requires partially demineralised apatite crystals that can grow as a result of exposure to solutions supersaturated with hydroxyapatite. It can be anticipated that the formation of an entirely new subsurface complex is unlikely, although it can occur on the surface areas exposed to numerous pH fluctuations (Park et al., 2011).

The effect of remineralisation can be enhanced with the use of fluoride. The previous thoughts on fluoride's mechanism of action were through systemic factors that changes the enamel structures pre-eruptively. There is a consensus that fluoride interferes with the caries formation locally. Hydroxyapatite dissolves at the same rate as fluorapatite formation when fluoride is available in the biofilm and the pH is more that 4.4 (Ten Cate, 2003). This causes a net decrease in enamel dissolution by recovery of calcium and phosphate ions which were lost as hydroxyapatite. This process is not considered as a true process of remineralisation where minerals redeposited is different from that which were lost. Fluorapatite is deposited on the surface while hydroxyapatite is dissolved from the subsurface. Fluoride is effective in retarding process since it is not influenced directly by factors of caries formation. The influence can be briefly explained through this graphic interpretation (Figure 2.7):

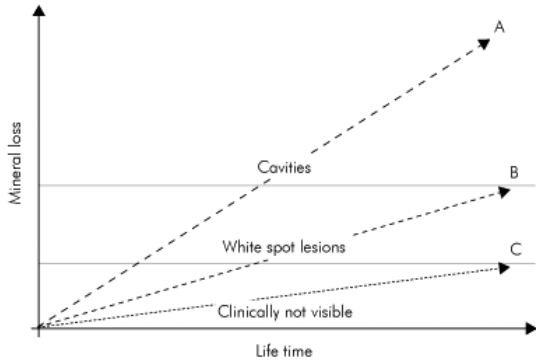

Figure 2.7 Influence of fluoride on mineral loss in a lifetime. (A) no fluoride. (B) under moderate caries activity. (C) under low caries activity (Cury et al., 2009)

2.4 Histopathology of Caries

2.4.1 Enamel White Spot lesions

The enamel framework is made-up of hydroxyapatite crystals which are arranged into long rods starting at the dentino-enamel junction and further extends into the crown in a wavy fashion (Roberson et al., 2006). The mineralisation process of these rods includes alternating periods of high and low activity levels. Low activity creates a rest line within the enamel rods and in combination with the rest lines of neighbouring rods, a striae of retzius is formed for which are identified by relatively greater organic content. The movement of hydrogen ions and water is permitted by the spaces in between the striae and prism boundaries' porosities acting like a molecular sieve, filtering the larger ions and allowing the passage of small ions. This filter-like behaviour describes the pulpal reaction prior to bacterial infiltration, because the movement of the ions can result in the actual cavitation of the enamel by acid dissolution of the underlying dentine. The greater permeability of the striae in the enamel surface causes lateral spread of enamel lesion by the pulpal response but of unknown mechanisms (Roberson et al., 2006).

2.4.2 Microscopic Features of White Spot Lesions

To develop a carious lesion, it may take a period of many months to even years as it is not simply a continuous and gradual loss of mineral, but more of a dynamic process that

entails a series of both demineralisation and remineralisation processes. Demineralisation is dissolution of the calcium and phosphate ions from the tooth into the plaque and saliva and on the other hand remineralisation involves the deposition of the calcium, phosphate and other ions from the saliva conversely into the previously demineralised tooth structure. When the rate of demineralisation exceeds the rate of remineralisation, then only by this condition, formation of lesion occurs (G. S. Kumar, 2015).

The WSL typically presents itself as subsurface demineralisation with an intact surface layer. The thickness of the surface layer varies from 10-30 microns, but microscopically these pores extend through the mature enamel to the point where the subsurface demineralisation has taken place. This point is where the main body of the lesion is located (Harris et al., 2004).

The WSL has been divided into four histological zones by Silverstone, namely (Silverstone, 1982)

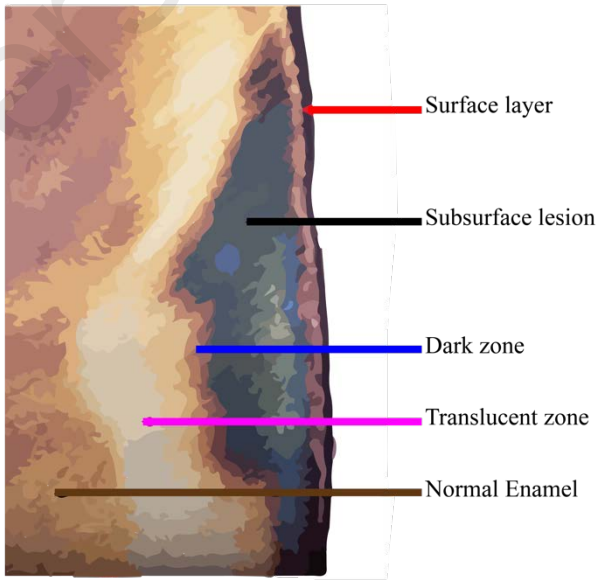

Figure 2.8 Schematic drawing of the white spot lesion that includes the translucent and dark zones, subsurface lesion (or body of the lesion), and the surface layer above the normal enamel.

a. **Translucent zone (Zone 1)**: Described as the advancing front of the lesion with slight demineralisation. It can be seen in 50% of the carious lesions
b. **Dark zone (Zone 2)**: Zone of active remineralisation and can be seen in a majority of WSLs
c. **Body of the lesion (Zone 3)**: this zone is on the periphery of the dark zone
d. **Surface zone (Zone 4)**: This is the outermost zone. It is also the zone of remineralisation.

2.4.3 Changes Seen at Ultra-Structural Level of a WSL

At ultra-structural level analysed using an electron microscope at a magnification of 3000x, the WSL presents a ragged profile, with pores extending into the enamel structure. The cariogenic acidic attacks may happen on the rods, between the rods, or both simultaneously (Harris et al., 2004). Micro-channels or pores have been observed in the surface zone that allow the access of acids into the subsurface layers, resulting in the removal of calcium and phosphorus ions.

In zone 3 of the lesion, demineralisation that occurs along the striae of Retzius appears progressive. Once the lesion reaches the dentino-enamel junction (DEJ), undermining of enamel occurs as a result of lateral spread of infections in the region that leads break down of the surface layer and this process progresses inwards (Harris et al., 2004).

2.5 Methods of Detecting White Spot Lesions

2.5.1 *In Vitro* Diagnostic Methods

Several analytical techniques have found utility for measuring dental mineralisation (Ten Bosch et al., 1991). Most of the techniques employed are *in vitro* techniques. These laboratory techniques have contributed to both the understanding of dental lesions and

the development of oral healthcare treatments. However, they are not readily amenable for use in clinical examination.

Additionally, none of the techniques currently used are suitable for the detection of individual stages of the lesion progression. Each methodology has its limitations and important considerations. Most of the conventional methods such as light or stereomicroscopic inspection, profilometry, transverse microradiography or polarised light microscopy used to measure caries do not establish the caries depth and severity as accurately *in vivo* as they do *in vitro* (Huysmans et al., 2004; Kim et al., 2011).

A study conducted by Schlueter et al concluded that profilometry was the most common quantitative technique to assess dentine and enamel not only *in vitro* but also in clinical studies (Schlüter et al., 2011). Surface hardness and microradiography were acknowledged as the next commonly applied technique for the evaluation of dentinal tissues.

2.5.1.1 Surface Profilometry

Surface roughness can be measured using contact (uses a diamond tip) or optical (uses a light beam) profilometers. In contact profilometry, a diamond tip of fixed radius 1.5–2.5 mm (El Karim et al., 2007) with varying shapes of the tip are used (Waterhouse et al., 2008). The tip used for detecting bumps on a surface is the chisel-point (0.25 μm x 2.5 μm) tip, while for surface roughness it is almost exclusively measured using the conical tips with a load that ranges from 0.05 to 100mg (Field et al., 2010). There is a risk of these tip causing damage to the specimen by the dragging motion across the surface measured (Barbour et al., 2004). To limit and minimise the effect, the recording speed of these contact profilometer is usually maintained at 1mm/s (Field et al., 2010). The vertical resolution is in the range as low as 0.1 nm for smooth surfaces or as high as 1 nm for rough surfaces.

Laser profilometers on the other hand uses a light spot aimed at the surface of the specimen, usually below 100 mm in diameter. Surface topography can be profiles from measuring the laser beam deselections, or with white light that utilises the confocal principle (Rodriguez et al., 2009). Colour and transparency can affect the results (Field et al., 2010). In a study done by Rodriguez et al in 2009, using laser profilometers at wavelengths of 785 nm on dental impression materials and stones, it was demonstrated that materials with darker colours had higher roughness values (Rodriguez et al., 2009). The laser profilometers have wavelengths that are absorbed by colours located at the same spectrum ends. The surface would not be scanned if an impression material absorbed colour at the same wavelength hence the reason why darker coloured impression materials showed higher roughness values (Field et al., 2010).

Table 2.1 Common Amplitude Parameters for Surface Measurement

No.	Parameter	Description
1	R_a	Arithmetic average of all deviations of the profile from the centreline
2	R_q	Geometric average of all deviations of the profile from the centreline
3	R_z	Mean of five roughness depths of five successive sample lengths of the profile
4	R_{max}	Largest of the five roughness depths
5	R_p	Height of the highest point above the centreline within the length of the profile
6	R_v	Depth of the lowest point below the centreline within the length of the profile
7	R_{pm}	Mean value of Rp in five consecutive sample lengths
8	R_t	Vertical height between the highest and lowest points of the profile within the evaluation length
9	R_{tm}	Mean value or R_{max} in five consecutive sampling lengths
10	R_{3z}	Similar to Rz except the individual roughness depth is the depth from the highest peak to the third lowest valley within the sample length

(Field et al., 2010)

The parameters or variants to measure tooth surface are summarised into a Table 2.1. These variants typically analyse and measure the average distance between the highest peaks and valleys of the profile and can also abbreviate some outliers, depending on the

engineering system involved (Field et al., 2010). It is challenging for untrained personnel to interpret the tabular form of the variants even with the help of modern engineering systems measuring the effects of surface change in the best possible way.

2.5.2 *In Vivo* Diagnostic Methods

WSLs are essentially characterised by mineral loss. Hence, this is a critical factor in the diagnosis and management of the consequent lesions. Clinically, the diagnosis of WSL has been primarily by visual evaluations, based principally on clinical assessments and review of radiographs (Bader et al., 2001). The WSL of smooth surfaces might be easier to detect visually, but in cases of approximal WSL, the situation can be challenging. Generally, caries and other dental abnormalities is primarily detected using dental X-ray imaging. This technique is used routinely to image dental structures and cavities within the oral cavity. Bitewing radiographs are commonly used to examine interproximal caries and recurrent caries. However, dental X-ray imaging has poor level of sensitivity for detecting early or incipient carious lesions and specially in WSL since the lesions are too shallow and do not provide enough definitions. Current clinical practice has been found to have restricted sensitivity and specificity at all stages of dental lesion progression and thus presents an obstacle to the effective practice of preventative dentistry (Gomez, 2015).

The average effective dose of a single bitewing equates to around 0.0003 - 0.0216 mSv. There is evidence that continual exposure to X-rays of some tens of millisieverts concentrated onto a small area is associated with an increased risk of cancer. On prolonged period of exposures, a publication by the UK Health Protection Agency stipulated a total lifetime cancer induction risk factor of 6.8% (for men) and 5.5% (for women) or simply to put it, 1 in 15,000 (for men) and 1 in 18,000 (for women) for every 1mSv effective dose received from dental radiographs (Keith et al., 2018). This is categorised in the lower risk category; however, it is important that each radiograph is

justified. The presence of possible detrimental effects from x-rays, suggest it might be imperative to venture and look into possible non-radiographic alternative methods to detect WSL.

2.5.2.1 Optical Coherence Tomography (OCT)

It is imperative that WSL are diagnosed as early as possible in its early stages prior to the development of frank cavitation (Karlsson, 2010). Optical Coherence Tomography (OCT) is recognised for providing non-invasive, visualisation of biologic microstructure based on the basis that the tooth has different tissue properties (Peters et al., 2001). With OCT, it is now possible to acquire real-time images with excellent axial resolution (Keith et al., 2018). The first documented *in vitro* images of both dental hard and soft tissue with OCT were acquired by Colston and colleagues in 1998 (Adriaenssens et al., 2017; Colston et al., 1998). Amongst the defects or anomalies able to be detected using the OCT are microleakages which can be readily viewed on OCT images as a clear line and gaps detection at the restoration interface (Machoy et al., 2017). OCT imaging may also rapidly detect voids of different sizes within a restoration (Dorri et al., 2015).

2.5.2.2 Introduction to OCT

OCT execute cross-sectional and volumetric imaging by gauging the magnitude and echo time delay of backscattered light. By transversely scanning the incident optical beam and performing sequential axial measurements of echo time delay (axial scans or A-scans) the images are generated in a two-dimensional (2D) data set representing the cross-sectional plane through the tooth tissue, achieved by capturing the optical backscattering of beams from the OCT (Drexler et al., 2008). B-scans or the obtained 2D images can be displayed in false colour, a natural colour rendition for aiding detection of features that are not readily distinguishable or grayscale to help visualize internal tissue structure of the tissue and its pathology. Three-dimensional (3D) data which contains comprehensive

volumetric data sets of structural information are generated by acquiring sequential cross-sectional images, scanning the incident optical beam in a raster or other two-dimensional pattern and can be further displayed similar to magnetic resonance (MR) or computed tomography (CT) images (Drexler et al., 2008).

OCT is an effective medical imaging innovation, due to the fact that it executes "optical biopsy," in real time, of in situ tissue microstructure and pathology, without the requirement of removing and processing specimens. Its use was pioneered in the field of ophthalmology and has spread into other specialties as well. The gold standard for assessing pathology is still by histological examinations, but it requires excision, fixation, embedding, microtoming, and staining of tissue specimens. The advantages of OCT over histological assessment are evident in several general clinical situations (Drexler et al., 2008):

a. Where excisional biopsy is dangerous or impossible.
b. Where conventional excisional biopsy has sampling errors.

2.5.2.3 Recent Advances in OCT

Throughout the last decade, OCT has been adapted enthusiastically by the interventional community, both for clinical and scientific applications with an exponential surge in the number of peer-reviewed manuscripts in the field reaching to almost 500 publications in 2016 alone. Recently, huge advancements can be seen in other medical fields but in dentistry not much has changed since the first attempts to use optical coherence tomography in 1998 (Adriaenssens et al., 2017; Colston et al., 1998) from the Laboratory of Medical Technology of Livermore, California, through collaboration with researchers from the University of Connecticut. In their initial discoveries, they presented the first prototype of a dental optical coherence tomography for *in vivo* application

designed to scan hard tissues to a depth of 3 mm and soft tissues to a depth of 1.5 mm respectively (Machoy et al., 2017).

Even though the first dental OCT prototype was developed by the Colston group, it was Feldchtein et al., in the same year who was the first to mention the possibilities of OCT to examine dental hard and soft tissues (Feldchtein et al., 1998). The group conducted clinical studies on the usefulness of OCT in the recognition of lesions of both soft and hard tissues of the oral cavity. In 2000, the same scientific centre identified and compared two OCT prototypes of different wavelengths of light: 850 and 1310 nm (Machoy et al., 2017). They concluded through the analysis of the quality of scans from individual devices and the evaluation of the possibility of reflecting the anatomical details, evidently, using longer wavelengths of light showed greater effectiveness (Adriaenssens et al., 2017).

In 2004, University of California in San Francisco became a leading centre dealing with OCT bringing forth a series of published articles, aiding knowledge on the aspects of OCT application in conservative dentistry (Machoy et al., 2017). In 2010, an innovative work using the potential of chitosan on enamel remineralisation was presented (Arnaud et al., 2010). The infiltration depth of chitosan into the enamel structure was evaluated by OCT. The attempt of complete enamel remineralisation was proven to be unfruitful, but the exploratory effectiveness of OCT as a diagnostic tool was once again validated.

Another facet of research using the OCT has become the assessment of dental restorations with composite fillings. The study (Braz et al., 2011) researched into the leakage of composite restorations and based on the analysis of OCT scans, fissure dimensions on average of 50μm could be effectively detected. The OCT with its high-resolution scans, is able to critically assess the structure of fillings. While evaluating gap formations under Class V restorations, Senawongse et al (Senawongse et al., 2011)

discovered the potential of OCT in the visualising the interface between the bonding system and the dentine, carious lesions analysis within the crown and root and also assessing secondary caries.

Hariri et al. in 2012 reported on OCT to evaluate light scattering and its magnitude and also investigated on the refractive indices (RI) of the enamel and dentine (Hariri et al., 2012). They were able to calculate the RI based on optical path length, real thickness, and OCT signal slope. They concluded that dentinal structures are anisotropic, and orientation of the tubules affects the RI unlike enamel (Hariri et al., 2012).

2.5.2.4 Types of OCT

(a) ***Swept-Source-OCT (SS-OCT)***

In mathematics, a Fourier transform decomposes a function of either function of time or a signal into its constituent frequencies. Fourier domain OCT (FD-OCT) functions by converting measurements from interfered light into physical delays or distances. FD-OCT is capable of measuring all the light from different delays while achieving axial resolutions nearing 2 μm (with advanced light sources), and image acquisition speeds of between 26,000 and 100,000 A-scans in current commercially available devices, or up to 1,700,000 A-scans in advanced FD-OCT prototypes. Currently, there are two commonly used applications of FD-OCT: spectral-domain OCT (SD-OCT) and swept-source OCT (SS-OCT).

SS-OCT utilises a tuneable swept laser that emits a “single” wavelength that sweeps across a broad range of wavelengths as a function of time. The interference spectrum is identified by a single photodetector or photodiode and digitised as the wavelength is swept. The A-scan rate of SS-OCT is set by the rate at which the light source is swept. SS-OCT devices generally uses wavelengths above 1000 nm and operating speeds equal to or greater than 100 kHz (Potsaid et al., 2010). The 2D cross-sectional images or B-

scans is generated by a point-by-point scanning of the OCT across a sample. B-scan can be stacked into a 3D image producing C-scans. OCT enables images that are generated from various scattering and absorption of light in different material components in both hard and soft tissues of the teeth. Interfaces of gaps, bubbles, restorations, and other defects can be seen as a contrast in the image.

However, as reported by Yun et al., there exist drawbacks of longer wavelengths where they are more readily absorbed by water (Yun et al., 2003). SS-OCT offers a slightly reduced image resolution relative to SD-OCT due to the need of using longer wavelengths in SS-OCT. The axial resolution in OCT imaging is directly proportional to the bandwidth of the light source used but in SS-OCT the bandwidth is limited by when light absorption by water is factored in.

2.5.2.5 OCT Applications in Dentistry

(a) ***OCT Dental Hard Tissue Imaging***

The transmission of visible light of 400–700-nm wavelengths through tooth substance are limited by marked light scattering (Colston et al., 1998). The relationship between light scattering in enamel and wavelength (λ) is defined as $1/\lambda$, where λ is the wavelength of the incident light (Wilder-Smith et al., 2008). Light absorption by water becomes a limiting factor for the absorption of infrared (IR) light at longer wavelengths exceeding 1,500 nm. Therefore, it was deduced that OCT imaging of the tooth best benefit at wavelengths of 700 and 1,500 nm, with excellent penetration up to a depth of 3 mm. In 2000, Otis et al. demonstrated the superior imaging and penetration of OCT systems using axial resolution of 12 μm with a 1,310 nm centre wavelength (Otis et al., 2000).

In 1998, Colston et al. presented the first *in vivo* optical coherence tomography (OCT) images of dental tissue (Colston et al., 1998) using an interferometer sample arm and transverse scanning optics built into a handpiece suitable for intraoral use. Diagnosis of

periodontal disease, evaluation of dental restorations, and detection of caries are few examples of the huge potential OCT offer in the imaging field of dentistry. Amongst the findings that were documented during this presentation were the average imaging depth of this system varied from 1.5mm in the soft tissues to 3 mm in hard tissues, axial resolution of 15 mm in a free space, lateral resolution of 50 mm and an average total lateral scan distance of 12 mm. Approximately 45 second for total scan time for each image. Further studies by this and other groups have clearly demonstrated the effectiveness of OCT for rapid, high-resolution imaging of dental tissues using OCT (Colston et al., 1998; Fried et al., 1995; Otis et al., 2000; Wilder-Smith et al., 2008).

(b) ***OCT Images of Restored Tooth***

Radiographic assessments and clinical examinations of restored margins are less than adequate modalities currently available to clinicians. OCT has shown to recognise precisely occlusal sealants and resin-based restorations. In a study conducted by Holtzman et al, a total of 21 qualified dental practitioners were asked to analyse OCT images of nine premolars and to identify whether it was not restored or either restored with sealant or composite restoration (Holtzman et al., 2010). Using a randomised blind protocol, the 21 dental practitioners with brief training period were able to distinguish restorations with composite and sealants with a sensitivity score of greater than 0.92 while the specificity of discrimination was greater than 0.94. Within clinically acceptable level, the dental practitioners were able to discriminate sealant treated tooth with a non-restored tooth at a sensitivity score of 0.88 and specificity score of 0.86. In this *ex vivo* study, the inter- and intra-rater reliability was also taken into consideration and revealed exceptional kappa scores of 0.82 – 1.0.

This authors also concluded that dental practitioners with no background of operating an OCT or interpreting an OCT image could be trained with a high degree of accuracy.

Using 3D OCT imaging, structural integrity and wear of composite resin restorations can be evaluated. Volumetric loss or surface changes is quantifiable using the OCT contour map of the restorative material over time. The estimation of wear can be determined by the traditional Moffa-Lugassy (M-L) scale ($r = 0.86$; $p < 0.05$).

(c) ***OCT Images of Root Canal Treatments***

In dentistry, OCT has also been useful in observing root perforations, intracanal anatomy, cleanliness of the root canal after preparation and detecting root cracks albeit thus far, it has only be limited to *in vitro* situations (Chen et al., 2021).

OCT is root canal treatments uses a very narrow optical fibre measuring 0.5 mm in diameter, with high-resolution capacities, enabling imaging of objects measuring a few micrometres and does not involve ionizing radiation. The imaging wire can be deployed independently or integrated into an existing therapeutic or imaging catheters. As it is flexible, it can easily fit into a prepared root canal and allows penetration through curvatures. The optical probe rotates inside the image vessel so that adjacent lines in each rotation compose a frame showing a cross-section of the tissue architecture in the wall. The scan is quick and takes 15 seconds for a 15-mm long root (Shemesh et al., 2007).

Although with few disadvantages such as the possibility of apical extrusion of the probe and relatively expensive use of disposable catheters, OCT imaging systems for root canal treatments is still promising and as it is still under development, more affordable versions could be available soon.

2.5.2.6 OCT and Other Imaging Techniques

OCT has functions that are closely related to ultrasound and microscopy. Despite OCT's limitation, whereby the light is highly scattered in most tissues resulting in potential imaging depths of only 2mm, its axial resolution ranging from 1 to 20 μm

equivalent to 10-100 times finer than standard ultrasound imaging. This high-resolution permit visualisation of tissue morphology. OCT thus bridges the gap between ultrasound and microscopy (Jang, 2014).

OCT's non-invasive and non-destructive attribute in real-time, high resolution and contrast, non-radiation imaging method are a few of the advantages of OCT over the other imaging options available currently. Table 2.2 shows a comparison between dental OCT and other dental diagnostic methods used today:

Table 2.2 Comparison of other dental diagnostic methods (Lakshmikantha et al., 2017)

Methods	Advantages	Disadvantages
OCT	1. High spatial resolution 2. Real time image 3. 3D image reconstruction availability	1. Limited penetration depth and scanning range
Radiography	1. Low cost 2. Broad measurement range	1. Radiative 2. Poor spatial resolution 3. Only 2-D image
Cone Beam-CT	1. Broad measurement range 2. 3D image reconstruction	1. No real-time image 2. Radiative 3. Poor spatial resolution
Intraoral digital camera	1. Low cost 2. Non-radiative	1. Surface information
Raman spectroscopy	1. High sensitivity 2. Responses to mineral and chemical concentrations	1. *In vitro* measurement 2. Expensive 3. No image
Laser fluorescence spectrometer	1. Real time detection 2. Responses to bacteria and chemical concentrations	1. Lack of diagnostic consistency 2. No image
Micro CT	1. High spatial goal resolution 2. 3D models acquisition 3. Short scan time	1. High radiation dose 2. Lots of storage data required 3. Artifacts are seen

Popular diagnostic methods today are radiography and dental computed tomography (dental CT). For better diagnosis, a three-dimensional image could be acquired from cone beam CT. Nevertheless, the ionizing radiation of radiography and dental CT limits their usage (Hsieh et al., 2013). Recently, several techniques have been developed for diagnosis of caries, such as a smart ultrasonic devices, LED-based dental optical probes, and laser fluorescence. Laser fluorescence spectrometers are considered as a dental caries detection and quantification tool (Hsieh et al., 2013), but their full application is still under investigation. Factors such as presence of bacteria, electrolytic solutions, and blood considerably influence the intensity of fluorescence spectrometers leading to problems due to lack of diagnostic consistency.

2.6 Managing Dental Caries

2.6.1 Caries Control Concept

For a long time, the term caries prevention has been considered synonymous with prevention by reducing the incidence of disease. In 1981 Fejerskov et al. promoted a new archetype on the mode of action of fluoride (Fejerskov et al., 1981). According to this new idea, fluoride does not prevent the advancements of cavities by forming protective mechanism of a more resistant enamel (Dirks, 1961) but rather exerts its cariostatic effect by interfering with the de-and remineralising processes during lesion development whereby it treats active caries lesions as they progress. As a consequence, fluoride was reformulated as a curative agent that operates by controlling the induction and development of dental caries at pre-cavitated stages of lesion formation. Classical caries epidemiologists declared that non-cavitated enamel lesions could not be reported with any certainty thus leading to the absence of clinical records. However, scrutiny of the original Tiel-Culemborg (Groeneveld et al., 1990) data on the effect of water fluoridation which in fact included observations of non-cavitated lesions showed that the new criterion was justified (Fejerskov et al., 1981). In 2003, caries lesion transitions analysis in a

controlled clinical trial of supervised brushing with fluoride toothpaste exhibited that fluoride promotes lesion arrest more than it inhibits lesion development (Nyvad et al., 1997), resulting in controlling (or delaying) the formation of cavities.

There is now a proposed shift from the concept of caries prevention to a broader evidence-based concept of 'caries control' when attempting to interfere with the dynamic processes of caries at all stages of lesion development. This is not merely a question about semantics. A more precise terminology should preferably be reflected for better promotion of dental health. The caries control concept developed gradually as it became obvious that the clinical criteria for assessing lesion activity were capable of predicting lesion outcomes and help clinicians in making informed treatment decisions. The caries control concept was successfully implemented in the cariology curriculum at Aarhus University as an integrated part of the course on restorative dentistry. The goal was that students should appreciate that a patient who disturbs the biofilm mechanically (brushing), chemically (fluoride), or by behavioural change (diet) is performing caries control (Anderson et al., 2011).

2.6.2 Conventional Management of Caries

A century ago, Dr G.V. Black, reported about his clinical successes in the prevention and treatment of smooth surface caries after recommending self-performed tooth-brushing (Black, 1910). Dr Black observed that his treatments were less effective at the cavitation stage. This may not come as a surprise because it is much more difficult to clean a carious cavity with undermined enamel than a smooth tooth surface. In deciduous teeth, where he had no suitable restorative material and small nervous patients who must not be frightened, he advocated opening the lesions to allow cleaning (Frencken et al., 2012).

Two decades later in 1938, Anderson published a case series of experimental arrest of 20 large occlusal dentine cavities following gross excavation of decay and elimination of margins of unsupported enamel that made the lesion inaccessible to biofilm removal. Anderson reported that the treated cavities experienced either partial or complete arrest of the carious process after the chewing function was re-established. Through these historical observations, and in addition to more recent clinical observations, it is implied when a plaque-free condition is clinically achieved, caries progression can be arrested at any stage of lesion development (Nyvad et al., 1997).

2.6.2.1 Arrest of Active Enamel Caries

Several clinical experimental studies have confirmed the original observations of Black (Black, 1910) . When active enamel caries lesions are cleaned regularly, the surface features change from chalky white to a more diffuse opacity, particularly in the peripheral shallow parts of the lesion. The total area of the lesion may be reduced and occasionally may completely disappear. It has also been suggested that localised ruptures of the surface layer of demineralised enamel may induce the formation of microcavities during lesion arrest. Altogether, these changes were interpreted to be mainly a result of surface wear (toothbrushing and mastication) rather than remineralisation of the demineralised tissue. The mineral uptake of the surface layer of the lesions differs from the inner porous layer because of restricted diffusion of ions in and out of the lesion. Therefore, it is improbable to 'repair' completely arrested lesions and they remain as lifelong whitish or brownish scars in the enamel.

2.6.2.2 Minimal Intervention Concept

Minimal Intervention Dentistry (MID) preserves the traditional, surgical manner of controlling dental caries, based on notion introduced by G.V. Black more than a century ago. MID is an ideology to ensure that teeth are kept functional for life. Without doubt,

contributions from the many studies on the effect of water fluoridation on caries development have greatly enhanced the development of the MID philosophy. The one study that attracted attention in terms of importance is the Tiel-Culemborg study from the Netherlands (Dirks, 1961). The outcome of this study, like many others, proved that water fluoridation enabled a reduction in the prevalence of cavitated lesions by roughly 50% and highlighting the importance retarding the progression of a carious lesion, rather than prevention of its development (Groeneveld et al., 1990).

The recent advancements of various adhesive materials and systems has aided greatly in fulfilling the primary aim of MID. The ability to reduce the need for cutting away healthy tooth tissues when using adhesive materials, which contrary to traditional restorative concepts, smaller and less destructive cavity preparations are needed when using adhesives and therefore, reducing the need for extensive removal of tooth structure (Peters et al., 2001). To the best of our knowledge, it was Mount (Mount, 1991) who first mentioned in his study the need for 'Minimal Treatment' of dental caries. Dawson and Makinson (Dawson et al., 1992a, 1992b), provided more elaboration and clarification and were the ones who first termed 'Minimal Intervention Dentistry' in their literature. Strategies of MID includes (Tyas et al., 2000):

1. Early caries detection and risk assessment
2. Remineralisation of demineralised enamel and dentine
3. Optimal caries preventive measures
4. Minimally invasive operative intervention
5. Repair rather than replacement of restorations.

2.6.3 Management of Non-cavitated vs Cavitated Caries

The beliefs of treating early carious lesions have shifted to a less invasive method. The efficacy of prophylactic schemes has been demonstrated in a systematic review

(Holmgren et al., 2014). The main criteria for the choice of a preventive or preventive and surgical approach is the presence or absence of clinical cavitation. Preventive approaches are advantageous and worthwhile in preserving the tooth surface integrity but necessitates early detection of non-cavitated carious lesions. Enhancing remineralisation in the non-cavitated primary lesions, preventive methods encompass tooth-brushing with fluoride toothpaste, dietary advice, application of remineralising agents (such as professional topical fluoride and CPP-ACP) amongst other have been found to beneficial (Frencken et al., 2012; Holmgren et al., 2014). Various combination of using micro-abrasion with remineralisation paste have been suggested to address cases of WSL. Micro-abrasion performed using silicon carbide micro-particles in soluble water paste and 6.6% hydrochloric acid (Ardu et al., 2007) and a paste containing casein phospho-peptide amorphous calcium phosphate complexes (CPP-ACP) are prime examples of materials used in this method. Every technique has limitations, and the major drawback of micro-abrasion is the amount of eroded enamel surface involved in the process.

Fissure sealant is an alternative preventive technique which can be used to treat and seal early occlusal pit and fissure caries in place and prevent its succession into deeper layers (Deery, 2013; Uribe, 2006). Studies has showed higher effectiveness in caries reduction, by using fissure sealant in occlusal surfaces compared to fluoride varnish (Beauchamp et al., 2008; Holmgren et al., 2014).

Micro-invasive approach such as caries infiltration have been introduced clinically to help manage approximal non-cavitated caries lesions in both sets of dentition stages. The technique's goal is to retard advancements of caries by infiltration of the lesion and sealing it. The usefulness of the intervention has been proven in approximal carious lesions in the primary dentition. Comparison to other non-invasive methods such as oral

hygiene habits and remineralising agents showed caries infiltration methods having superior preventive effects (Dorri et al., 2015; Martignon et al., 2012).

The infiltration technique has several benefits over the other techniques. Firstly, the amount of dental tissue removed are less and secondly deeper subsurface lesion that are retarded for remineralisation, improves aesthetics as well (Paris et al., 2009).

Misdiagnosing a lesion could lead to an unwarranted irreversible removal of tooth tissue and cavitation. Within the limitations, other intervention modalities should be explored to minimise loss (Almutairi, 2017). Taking into consideration the conventional approaches, there are five main management strategies to be used in irreversible cavitated teeth situations (Innes et al., 2016):

- **Complete caries removal** (non-selective removal of hard dentine) followed by restoration.
- **Partial caries removal** followed by restoration. Partial caries removal can be performed using selective removal of soft dentine or stepwise removal of dentine. Stepwise excavation starts selective removal to soft dentine and followed by selective removal to firm dentine 6-12 months later.
- No caries removal and seal the lesion in place with restoration, for example, Hall technique.
- No caries removal, prevention with/without making the lesion cleansable. The tooth may not be restorable. This approach reported good results in arresting caries and high acceptability (Santamaria et al., 2015).
- Extraction.

2.6.4 Approximal Caries Infiltration Studies

A novel micro-invasive technique of infiltrating TEGDMA-based materials into a tooth surface with porosities to block progression of caries was introduced bearing the name ICON® (infiltration concept) and has been commercially available since 2010. This formulation was created with the intent to treat interproximal and anterior WSL.

The emergence of bonding agents and further advancements of sealants have seen numerous studies done on the treatment of incipient caries since. When it comes to the concept of infiltration, the literature is very limited. The earliest known research conducted on the concept of infiltration was conducted by Robinson et al in 1976 (Robinson et al., 1976). Resorcinol formaldehyde, an adhesive compound, was selected because of it had properties such as being bactericidal, low viscosity, hydrophilic, mechanically adept, and aesthetically pleasing (Robinson et al., 1976). In the experiment, extracted human molars with WSL were selected and infiltrated with resorcinol formaldehyde and polymerized. After experimenting with a few etchants, it was found that the penetration of the resin was greatly increased when etched with HCl for 5-10 seconds. Other significant findings were that 60 ± 10% of the lesions pore volume had been occupied by the resin which concurred with findings from the histological section and presence of pores increased 300% in the control group when compared to treatment group after subsequent demineralisation (Robinson et al., 1976).

Robinson et al found resorcinol formaldehyde to be clinically unacceptable as only 60% of the lesion pore volume had been occluded (Robinson et al., 1976). In a similar study by Robinson et al., many years later, Scotch Bond™ (3M Dental products), Gluma® 2000 (Bayer Dental, Germany), All-bond (Bisco Inc., Ill), Amalgam bond (Parkell Biomaterials, NY) and cyanoacrylates were all tested and analysed (Robinson et al., 2001). The study concurred with his previous findings in that not only resorcinol

formaldehyde, but all the resin materials including other resin dental bonding systems had the potential to infiltrate into lesions and protect them from secondary acid attacks (Robinson et al., 2001). Gray et al, evaluated the extent of infiltration with a polymerizable resins it carious lesions (Gray et al., 2002). The 2002 *in vitro* study was done on extracted human pre-molars and the surface treatment was done using Scotch Bond™ and Seal & Protect™. Gray and Shellis further subdivided the groups according to different etching times and found the percentage of penetration of a resin material in influenced by the duration and number of times etched (Gray et al., 2002).

In 1983, an *in vitro* study done by Rodda using human third molars evaluating the intake of multiple dental resins into artificially induced carious lesions (Rodda, 1983). The materials were methyl-methcrylate (Sevitron™), and different diacrylates that were activated chemically, or light cured; Delton® fissure sealant (Johnson and Johnson dental products) and Adaptic Bonding agent™ (Johnson and Johnson dental products) Nuva seal™ (L.D Caulk Company) and Visio-bond™ (Espe, Seefield, Germany). Amongst the findings, the methyl-methacrylate was the only material that failed to penetrate any lesions. The penetration depths varied for all of the other resins infiltrated into the body of the lesion (Rodda, 1983).

Further studies were conducted to analyse the potential of resin infiltration. Goepferd et al, tested the resistance of WSL to acid attacks after etching with phosphoric acid and infiltrated with a resin material (Goepferd et al., 1989). Comparison was done between treated WSL and WSL with no resin interventions. The findings revealed that the resin treated area progressed less when compared the baseline (mean lesion depth=67 microns) and progressed lesions (mean lesion depth=100 microns), but the new lesions around the resin treated (mean lesion depth=57 microns) areas progressed less than the treated areas (mean lesion depth=60 microns). This explains why the sealed sound enamel adjacent to

the white spot lesions did not undergo demineralisation indicating protection by the resin tags (Goepferd et al., 1989).

In 1997, another study on resin infiltration was done by Garcia-Godoy et al, assessing the progression of WSL sealed with unfilled resin (Garcia-Godoy et al., 1997). Findings from the study showed initial caries progression was up to a depth of 366 microns. After the secondary acid attack, the depth of lesions in areas of frank cavity versus the treated areas were 746 microns and 298 microns respectively. Garcia-Godoy et al concluded that there was enough evidence to show the efficacy of unfilled resin in sealing WSL (Garcia-Godoy et al., 1997).

Interestingly enough, all of the above studies of the infiltration technique were conducted *in vitro*. The effectiveness of resin infiltration was also described in studies involving clinical settings. An example of such study was done by Clarisse Abuchaim et al, in 2010 at the University of Oeste De Santa Catarina, Brazil. In this study, they treated active approximal caries lesions and evaluated the effectiveness of sealing it with an adhesive system after one year (Abuchaim et al., 2010). Subjects were divided into control (no treatment) and experimental group. The subjects in the treatment groups received 35% phosphoric acid as the etching component followed by an adhesive (OptiBond Solo, Kerr, Orange, CA, USA). Reviews were made at two time points, six months and at the end of one year. With the aid of radiographs, the caries progression rate was analysed, and the findings were lesion regression, no changes and lesion progression were 22%, 61% and 16% for the experimental group. In the control group, regression, no change and progression were observed in 27%, 36% and 36% of the subjects, respectively.

In the few studies described the potential of various infiltration materials (resins) in slowing down or inhibiting progression of lesion showed excellent results. Despite many

in vitro studies demonstrating promising results, the numbers of clinical studies assessing the efficacy of simulating *in vivo* delivery of the materials *in vitro* are still low.

2.7 ICON® (Infiltration Concept)

2.7.1 Rationale and Protocol for the Treatment of Approximal WSL

In 2008, a new treatment concept by the name of ICON® was introduced. ICON®, an abbreviation for Infiltration Concept was later made available commercially to treat cases of WSLs in 2010 (Gray et al., 2002). This minimally invasive technique was initially used for WSL of the approximal surfaces of the teeth.

Enamel lesions are a frequent occurrence and can be attributed as a result of long-term inability to clean these areas especially the approximal tooth contacts. A simple interpretation is when plaque accumulates, caries form (Paris et al., 2009).

ICON® is a caries infiltration technique and an alternative therapeutic approach to prevent the further progression of enamel lesions. The main purpose of ICON® is to obstruct the porosities as a result of demineralisation in the body of the WSL using a low viscosity light-cured resin that has been developed for infiltration into the porous subsurface enamel (Paris et al., 2009). ICON® have low viscosity and low contact angles to the enamel, but a high surface tension for optimal penetration into the body of lesion. The material was developed at the University of Kiel, Germany after a series of pilot tested using various mixtures and ratios of resin materials such as TEGDMA and BisGMA to name a few. The ICON® penetrates into the lesion with the aid of capillary forces.

In a single ICON® package, an infiltrant, additives and initiator, acid conditioner, and ethanol are included. The major components of ICON® are tetra-ethylene glycol dimethacrylate (TEGDMA) – the major component of the infiltrant, 15% hydrochloric

acid for the acid conditioner and ethanol as the dehydrating solution. ICON® has a refractive index (RI) (1.46) close to sound enamel (1.62). The whitish appearance of WSL is due to the differences in the RI within the body of lesion generally filled with either watery medium (1.33) or air (1.00). When the porosities are infiltrated with ICON, the differences between the enamel and the infiltrated porosities are negligible, making the lesion appear similar to its surrounding (Paris et al., 2009).

2.7.2 Recommended Application Protocol

Resin infiltration aims to fill the voids in the subsurface enamel caused by mineral loss. Infiltration of a low viscosity resin into incipient caries lesion may effectively prevent the diffusion hydrogen ions into the tooth during an acid attack, thereby inhibiting caries development and progression (Meyer-Lueckel et al., 2008; Paris, Hopfenmuller, et al., 2010; Robinson et al., 2001).

Pre-Infiltration Etching. WSLs often have a thin hyper-mineralised enamel surface (approximately 30 microns) that has a smaller pore size than the demineralised subsurface (Bergman et al., 1966). This outer enamel veneer prevents the infiltration of light-cured resins, a process driven primarily by capillary action (Robinson et al., 2001). To open these pores, an acid is used. Meyer-lueckel et al., showed that the use of 15% hydrochloric acid (HCL) is more potent than the more common pre-restorative etchant, 37% phosphoric acid (H3PO4) (Meyer-Lueckel et al., 2007). They measured resin penetration depth in human enamel sections with natural WSLs following treatment with 15% HCL gel, 37% H3PO4 gel, or no acid treatment. Treatment with 15% HCL for 120 seconds allowed the infiltrative resin to penetrate to a mean depth of 58 μm, while 120 seconds of H3PO4 and no acid treatment showed penetration of 18 and 0 μm, respectively.

The Infiltrative Resin. The penetration coefficient (PC) measures the ability of a liquid (in this case, a low-viscosity, unfilled resin) to penetrate into a porous material

(e.g., demineralised tooth structure). PC is the rate of penetration of a liquid into a capillary space in centimetres per second. The PC of an infiltrative resin is directly related to its surface tension and viscosity. The higher the surface tension and the lower the viscosity, the greater is the resin's ability to penetrate into a caries lesion. Paris and colleagues in 2007 calculated the PCs of five commercially available adhesive resins, five commercially available fissure sealant resins, and 66 experimental composite resins. The authors concluded from their findings that the highest PCs in resins contains triethylene-glycol-dimethacrylate (TEGDMA), 2-hydroxyethyl methacrylate (HEMA), and 20% ethanol (Meyer-Lueckel et al., 2008; Meyer-Lueckel et al., 2007; Paris et al., 2009; Robinson et al., 2001; Robinson et al., 1976; Rodda, 1983).

$$PC = \frac{\text{(Surface tension of liquid) x (cosine of the contact angle)}}{\text{2 x (viscosity)}}$$

Inhibition of Caries Progression. As previously discussed, diffusion of acid into the teeth and mineral ions out of a caries lesion occurs through enamel pores. If these pores were to be occluded with resin, ion diffusion would effectively stop and thereby arrest the caries process (Kidd et al., 2016; Mertz-Fairhurst et al., 1998).

2.7.3 *In Vitro* Studies with ICON®

An *in vitro* study done by Paris et al evaluated four experimental resin materials (PC63, PC185, PC204, PC391) of different penetration coefficient in inhibiting advancements of approximal WSL. No significant difference among all 77 teeth in groups tested at baseline. After storing the specimens in the demineralising solution for 200 days and subsequently for 400 days, higher demineralisation was seen in the negative control and 2 resin groups (PC63, PC185) compared to the baseline readings. The remaining 2 resin (PC204, PC391) group showing no significant changes after 200 days, but after 400 days,

the mineral loss in PC204, PC391 and positive control was the lowest compared to all the other groups (Paris & Meyer-Lueckel, 2010).

In a study conducted by Meyer-Lueckel et al, ICON® was compared to a commercially available adhesive evaluating the penetration co-efficient of the materials *in vitro* (Meyer-Lueckel et al., 2008). The findings of the experiment showed that the mean maximum lesion depths were comparable for both the groups but the mean for maximum infiltration depth and percentage was substantially higher for the ICON® in comparison to the adhesive (Meyer-Lueckel et al., 2008).

Subramaniam et al., in 2014 quoted "The partially mineralised intact enamel surface layer could hamper the resin from penetrating into the lesion. Hence, this layer has to be removed using acid etching with 15% hydrochloric acid gel" (Subramaniam et al., 2014). This was in agreement with an earlier study in 2007 by Lueckel et al which tested and compared the efficiency of three different surface layer removing acid gels (37% phosphoric acid (H_3PO_4), and 2 experimental hydrochloric acid (HCL)) (Meyer-Lueckel et al., 2007). According to their findings, 15% HCL with etching time of 90 and 120 seconds showed significant surface layer reductions when compared to those etched with the 37% H_3PO_4 and further proved the efficacy of using 15% hydrochloric acid over the 37% phosphoric acid in surface erosion thus creating porosity enabling infiltration.

The treatment of cavitated lesions is still relatively uncertain. Paris et al., conducted an *in vitro* experiment to study cavitated lesions on the approximal surface of premolars treated with the resin infiltration method (Meyer-Lueckel et al., 2007). The objective of this study was to gauge and assess infiltration patterns of approximal carious lesions. From the study, the obtained median lesion depth of all the specimens was 961 microns in the enamel, with increasing porosity in the dentine. The resin infiltration penetrated deeply in all the demineralised parts, with no significant difference in percentage of

infiltration of demineralised enamel. They concluded, with increase cavity depth, width and area is reflected with an increase in ICDAS code. For ICDAS 3, 4, and 5 cavities, resin infiltration was absent or significantly lower compared to a code 2.

2.7.4 Clinical Studies with ICON®

An *in vivo* experiment to evaluate masking of labial enamel using the resin infiltration method was conducted by Shin-Kim et al from the Department of Paediatric Dentistry, Pusan National University (Kim et al., 2011). The goal of this study was particularly to clinically evaluate the efficacy of the resin infiltration technique in masking WSLs. Eight out of twenty teeth with developmental defects remained unchanged and from that they concluded that some of the cases had colour that were too dramatic to mask and longer duration of studies are needed to assess differences.

The feasibility of sealing early proximal caries and halting was confirmed by a clinical study involving an eighteen-month split-mouth experiment conducted by Martignon et al, in 2006 (Martignon et al., 2006). Test subjects received treatment with either Gluma® One Bond Adhesive (Heraeus Kulzer) or Concise Sealant (3M ESPE). The final outcome showed that 30 (43%) of the test, and 59 (84%) control lesions had progressed ($p<0.001$, 95% CI: 28-56%). According to the author, despite caries progression, treated teeth fared better and concluded that it was feasible to seal early approximal caries. In 2010, a radiographic study evaluating the progression of lesion after infiltration using a randomized split-mouth placebo-controlled trial was carried out by Paris et al. The main purpose of this experiment was to assess the effectiveness of the method of resin infiltration into the approximal lesions compared to that of non-operative measures solely with regard to the progression inhibition (Paris, Hopfenmuller, et al., 2010). The results revealed that 37% of the lesions in the placebo group showed caries progression and only

7% treated with ICON® were affected. From the results and findings, the authors were able to infer the benefits of ICON® infiltrations.

Another example of a clinical split mouth experiment is a study conducted by Ekstrand et al, in 2010 with a goal to evaluate the efficacy of resin-infiltrated caries lesion covered by fluoride varnish with that of fluoride varnish only after a period of 1 year (Ekstrand et al., 2010). The results showed that after one year, progression of the lesions was noted in 31% of the test lesions and 67% based on the ICDAS score. Radiographically, these caries progressions were noted in 23% of the test and 62% of the control lesions. The authors were able to deduce that using resin infiltration in combination with fluoride varnish showed significantly promising results.

Since the first known concept of caries infiltration introduced by Robinson et al, in 1973, groundworks were set in motion for further evolution of the infiltration materials and methodologies in treating non-cavitated lesions. In most if not all these studies, have come to a consensus that resin infiltration materials are most promising and beneficial and a viable method in prevention and early treatment of dental caries. Previous work on resin infiltrations has led to the development of ICON® at the University of Kiel, Germany. Several *in vitro* studies were conducted to develop and create the ICON® infiltration material.

Not only have researchers found out that ICON® can be used to treat WSL of varying degree but in recent clinical studies suggested the benefits also includes colour masking in teeth with developmental defects or post orthodontic treatment. Many studies concurred that ICON® is effective in preventing development of the caries lesion, in comparison to no treatment. In clinical studies involving radiographs, it has shown the progression of the lesion can be distinguish with the help of radiographic imaging. With respect to promising results presented in these studies, it is most important to take into

consideration, that even though the idea of resin infiltration has been around for quite a while, the ICON® which is currently the standard of resin infiltration, is relatively new. Clinical studies with longer follow-up period are required to come to a conclusion regarding ICON®.

Limited studies have been done to compare the ICON® material with topical fluorides *in vitro* simulating an *in vivo* method of application. The present study is an *in vitro* study conducted with an aim to compare ICON® with a topical fluoride in prevention of demineralisation through an *in vitro* method that mimics an intraoral application of the materials.

CHAPTER 3: MATERIALS AND METHODS

3.1 Ethical Approval

The use of human teeth for scientific purposes was approved and in accordance with the ethical guidelines set by the Ethics Committee/IRB, University of Malaya (**Reference number: DF RD1927/0090 (P)**).

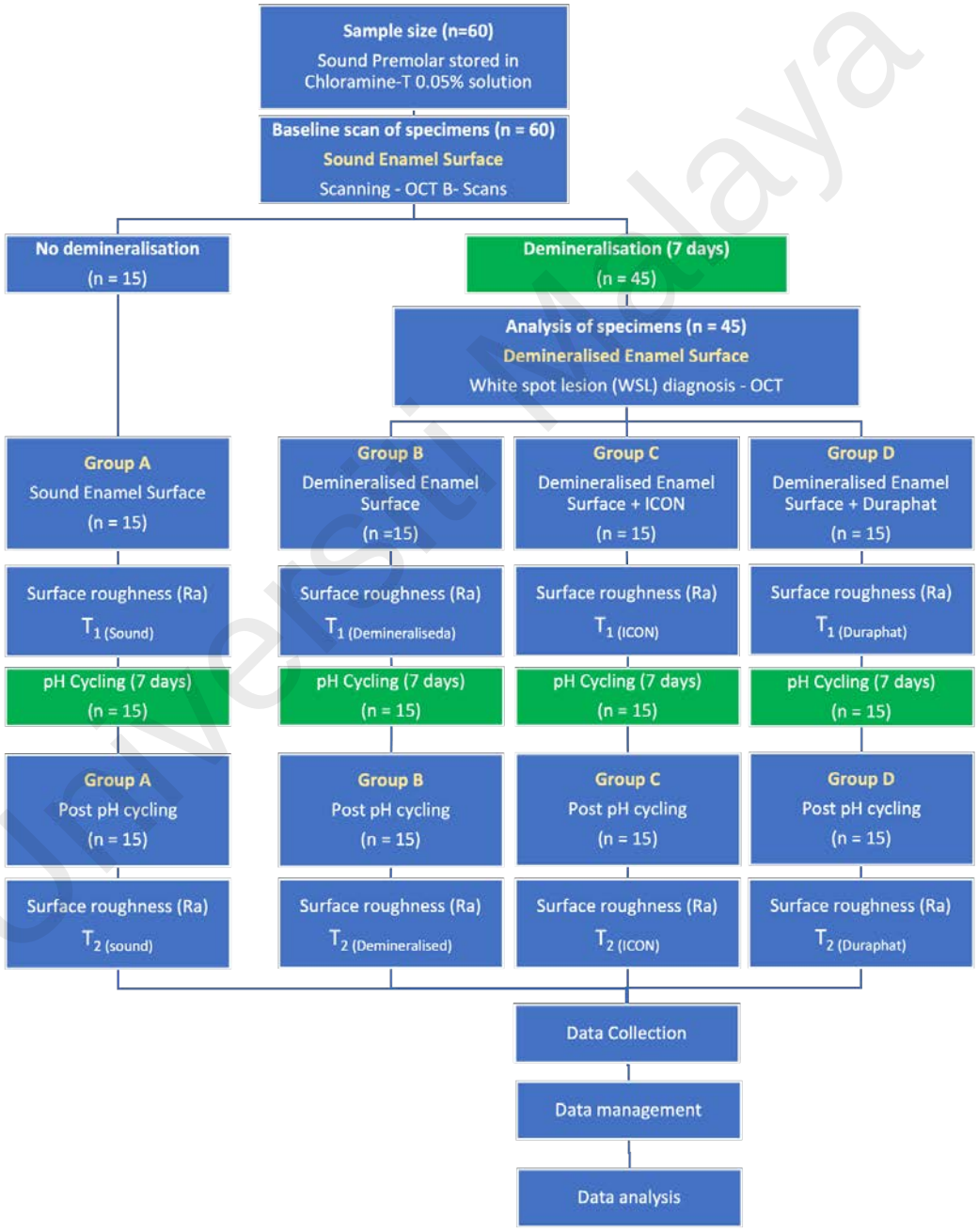

Figure 3.1 Flowchart of the research methodology

3.2 Research Methodology

3.2.1 Sample size calculation

A sample size of sixty sound permanent maxillary and mandibular human premolars was determined for this study with 15 teeth in each group. Sample size was computed at $\alpha = 0.05$ and effect size of 1.67 (Arslan et al., 2015). A sample size of eleven was required to get a statistically significant difference after treatment with a power of 95% after secondary demineralisation and a sample size of nine was required to have a power of 90%.

3.2.2 Sample Collection

Sixty extracted sound permanent maxillary and mandibular human premolar teeth were obtained from private dental clinics and dental institutions from around the Klang Valley, Malaysia were used as specimens for the initial step of demineralisation. The teeth were cleaned to remove debris and blood and disinfected in 0.5% chloramine solution for 1 week (Armstrong et al., 2017). They were then cleared of any leftover debris and residues with a prophylaxis brush and pumice powder. The teeth were stored in distilled water at a temperature of 37°C before the start of the experiment.

3.2.3 Pilot Studies

Pilot studies were done not only to better understand the process and materials involved, but also to comprehend the evaluation and analytical procedures in order to eliminate potential limitations. Specifically, the methods of lesion creation, treatment procedures, diagnosing WSL under the OCT, analysis of surface roughness and microhardness were critically assessed.

In review of published articles, WSL creation were usually predictable and successful but the method of scanning using the OCT are subjective to a certain extent. Thus, to

determine the final materials and methods, extensive series of pilot testing were done to better understand and finalise the definitive experimental protocols.

Since OCT is only used to determine the absence and presence of WSL of at least 120 microns, a series of OCT images were taken, and inter- and intra- reliability test were conducted. The overall intra-rater percentage of agreement and kappa statistics were 93% and 0.81 respectively. The overall inter-rater percentage of agreement and kappa statistics were 88% and 0.76 respectively.

An array of the demineralising solution with a pH ranging from 4.0 – 5.5 were used in previous studies on to create artificial WSLs. Immersion of the teeth in solution with pH of >4.6 for 6 days was not sufficient to create a non-cavitated white spot lesion with a depth of at least 120 microns. Minimal to no significant changes were observed when viewed under OCT. The pH of the solution in this study was adjusted to 4.5 and after 6 days, the teeth had lesion depth of within 120 – 200 microns.

3.2.4 Specimen Preparation

Application jigs (Figure 3.2a) for maxillary and mandibular study models were fabricated out of epoxy resin with missing second premolars and first molars in each quadrant. The 'missing' teeth/empty slots in the epoxy models were replaced with an artificial tooth in the molar slots and specimens in the premolar's slots. For each empty slot, a tooth was embedded into a polyvinylsiloxane putty (Flexceed®, GC Dental Products Corp., Japan) prior to placement into the slot. The orientation of the tooth was adjusted to simulate intraoral contact between adjacent teeth (Figure 3.2b). The contact point dimensions were adjusted (Figure 3.2c) to not exceed 3mm buccolingually and 2mm occluso-gingivally (Gohil et al., 1973). The consistency of proximal contact was registered as a "snap" when the floss was passed through the contact point. Upon setting,

contact points and area of demineralisation were determined and the putty was numbered accordingly.

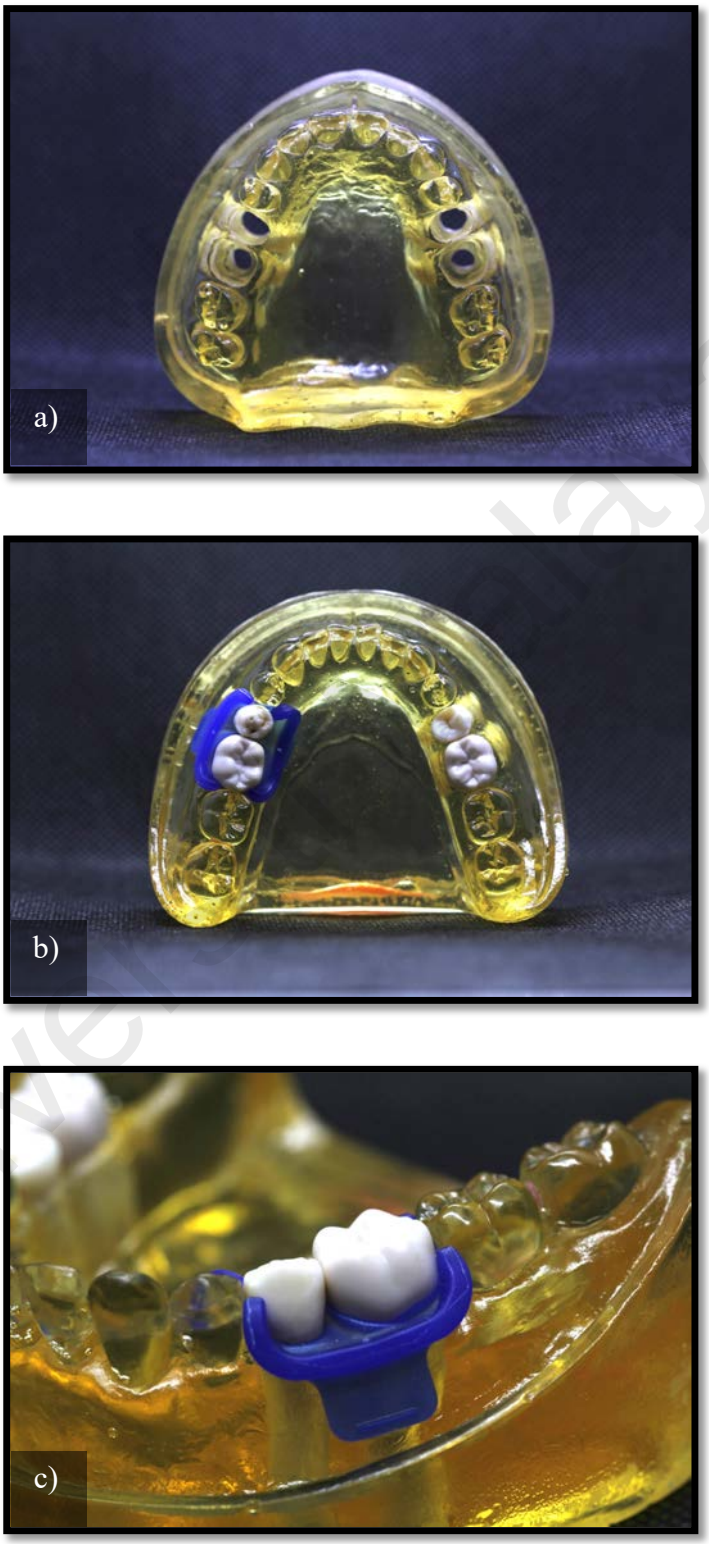

Figure 3.2 Application jig a) Prefabricated slots for placement of specimen and a controlled artificial molar b) Occlusal view of specimens and controlled artificial teeth in place with rubber dam c) Lateral view of the jig with specimen

3.2.5 Sample Preparation

The working window preparation (Figure 3.3) were made for all the specimens prior to baseline OCT scans and initial demineralisation. The teeth were taken out of the storage media and thoroughly cleaned by placing in distilled water. Custom-made round stickers were pasted onto the pre-determined area of demineralisation. All the surfaces of the specimens were completely painted (2 layers) with an acid-resistant nail varnish (Essence, New York, USA). Upon the nail varnish drying, a tweezer was used to remove the sticker leaving a circular window with a diameter of 3 mm in the centre of the proximal surface and 1 mm under the pre-determined contact area of each tooth. This established circle seen at the centre of the tooth was then ready to be scanned under the OCT for a baseline scan.

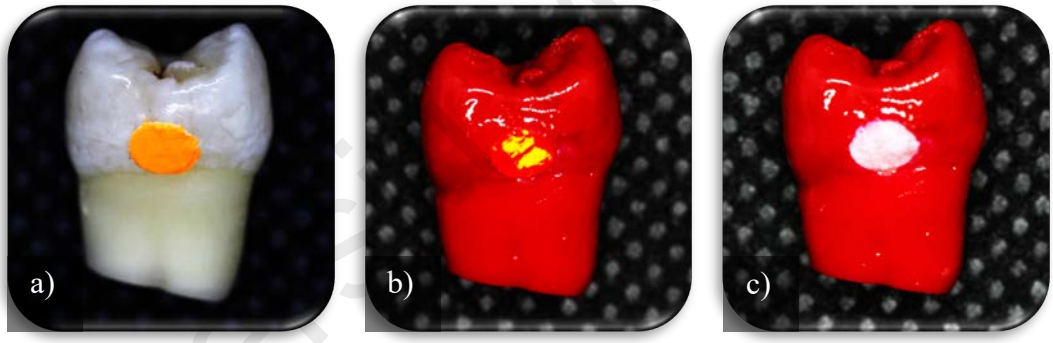

Figure 3.3 Working window preparation a) A custom made sticker is placed on to the proximal surface b) Nail varnish is painted completely over the tooth c) Upon the nail varnish drying, the sticker was removed leaving a 3 mm in diameter working window

3.2.6 Optical Coherence Tomography Scanning (Baseline)

For analysis of enamel changes under optical coherence tomography (OCT), customised individual PVS putty jigs were prepared for all the specimens and numbered from 1 to 60. Specimens were placed in customised jigs for proper placement and orientation and subsequently a baseline OCT B-scan was taken for each of the 60 specimens.

The baseline B-scans for all the specimens were done using the swept-source OCT (Thorlabs OCS1300SS, Thorlabs Inc, New Jersey, USA) (Figure 3.4). Prior to analysis, each of the specimens were washed with distilled water and fixed on a micrometre metal stage tilting 5°. The B-scan images were acquired using a standard parameter for all specimens (Table 3.1).

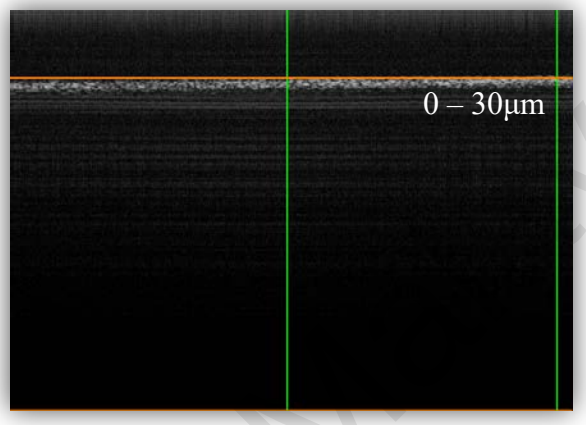

Figure 3.4 Baseline B-scans of proximal tooth surface of premolars with minimal (0-30µm) surface demineralisation.

Table 3.1 Parameters for optical coherence tomography

a.	Centre wavelength:	1310nm (1260-1360nm)
b.	Bandwidth:	214nm FWHM
c.	Sensitivity:	≤ 106dB
d.	Axial/lateral resolution:	<7.5 (air)/15.6µm
e.	Field of view	3.0mm (width) x 1.84mm (depth)
f.	Imaging speed	48kHz

3.2.7 Experimental Groups

The specimens were equally divided into four groups using a random integer generator and groups received equal numbers of maxillary and mandibular teeth. In a systematic order, the specimens were assigned to sound (Group A), demineralised (Group B), ICON® (Group C) and Duraphat® (Group D) groups. The specimens were renumbered according to the assigned groups (Table 3.2). Floss was tied at the root ends of the teeth,

and the ends of the floss were color-coded with a sticker to identify the assigned group. Specimens were stored in distilled water at 37^0C when not being manipulated.

Table 3.2 Randomised grouping of specimens

	Group	Number
Sound	A	1 - 15
Demineralised	B	16 – 30
ICON®	C	31 – 45
Duraphat®	D	46 - 60

3.2.8 Initial Demineralisation

The first cycle of demineralisation was conducted to create initial interproximal WSL for Group B, C, and D. The demineralisation protocol was carried out in a standard acid-buffer demineralisation solution without fluoride (Ten Cate et al., 1988). The solution contained 2.2 mM calcium chloride, 2.2 mM potassium meta-phosphate, and 50 mM acetate buffer. All the teeth were suspended in the acid buffer demineralising solution with a pH of 4.5 for 7 days (Figure 3.5) Upon removal of the specimens from the solution the specimens were visually inspected. The resulting white spot lesions (chalky white appearance) were further analysed under OCT.

Figure 3.5 Tooth was tied individually with dental floss and suspended in a demineralising solution

3.2.9 Optical Coherence Tomography Scanning (White Spot Lesion)

The scanning protocols for Group B, C, and D specimens (Figure 3.6) were similar to baseline scanning.

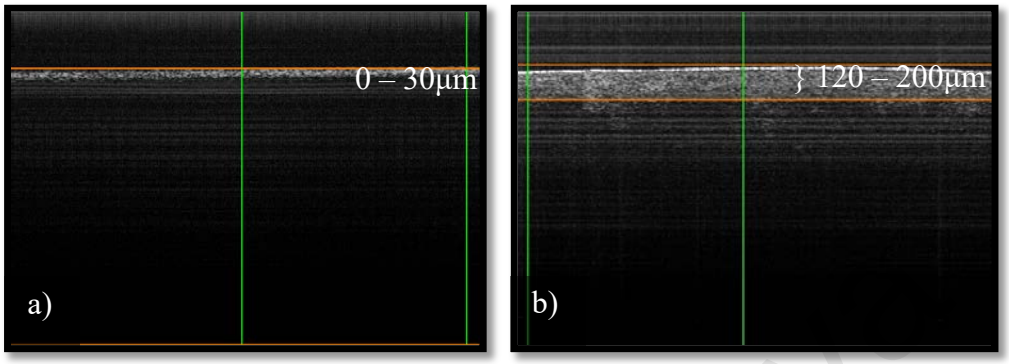

Figure 3.6 OCT B-scans. a) sound proximal surface of tooth structure, b) artificially induced white spot lesion of 120 – 200µm depth measured using Thorlabs Inc software measuring ruler

3.2.10 Surface Roughness Measurement

Group A and B

The control groups (A – negative control and B – positive control) did not receive any interventions and served as a comparison group for the other two treatment groups. These specimens without any interventions were embedded into epoxy resin (Hard Epoxy Resin, Ezlaser, Malaysia) of a 3:1 resin to hardener weight ratio, with the area of demineralisation exposed and as parallel to the scanning possible prior to surface roughness analysis (Figure 3.7).

Figure 3.7 Specimens that were embedded into epoxy resin prior to surface roughness analysis

All 30 teeth assigned to these two groups were analysed in a similar fashion, under similar conditions at room temperature and humidity. Surface roughness measurements were taken using a non-contact profilometer 3D Alicona, (Infinite Focus G4 microscope, Alicona Imaging, Grambach Austria) and the average surface roughness (R_a) were recorded for each specimen. 3D images of the proximal enamel surfaces (80×80 µm in size) of the area of analysis were also obtained.

Group C (ICON®)

With the specimen seated in the application jig, the demineralised teeth were infiltrated with Infiltration Concept (ICON®). The treatment kit is shown in Figure 3.8. Each tooth required approximately 10 minutes to complete etching and infiltration. The infiltration of all teeth in this group was completed in at least two sessions over two days.

Figure 3.8 ICON® Proximal treatment kit

A mini dam was used to isolate the tooth and a wedge, provided in the kit, was used to create space interproximally. A floss was used to gauge the space of around 50 µm, adequate for infiltration with ICON®. ICON® Etch, a 15% hydrochloric acid gel was administered on to the lesion via the green side of the special proximal tip supplied in the kit. Only the green side of the proximal tip can dispense the etchant. The lesions were etched for three minutes each, rinsed under running water for 15 seconds and air-dried with moisture-free air for 30 seconds. The specimens were further dried with ICON® Dry,

using a dispense tip and left undisturbed on the surface for 30 seconds. The surface was again air-dried at approximately 5 cm away with moisture-free air for 30 seconds.

The next step involved the application of the ICON® Infiltration, on to the surface of the lesion via a new Proximal® tip (Figure 3.9). The resin material was dispensed (2 turns) and a floss was used to spread the material evenly on to the proximal lesion. The material was allowed to stay on the lesion for three minutes. After three minutes, visible excess resin material was removed using a new floss and a cotton swab pinched by a tweezer and the material was light cured (Cure Rite Denstply Caulk, DE, USA; Light output: >450nm) for 40 seconds. ICON® Infiltration was re-applied, left for two minutes, and excess material was again removed in the same manner before exposing the site to a second light-curing for another 40 seconds.

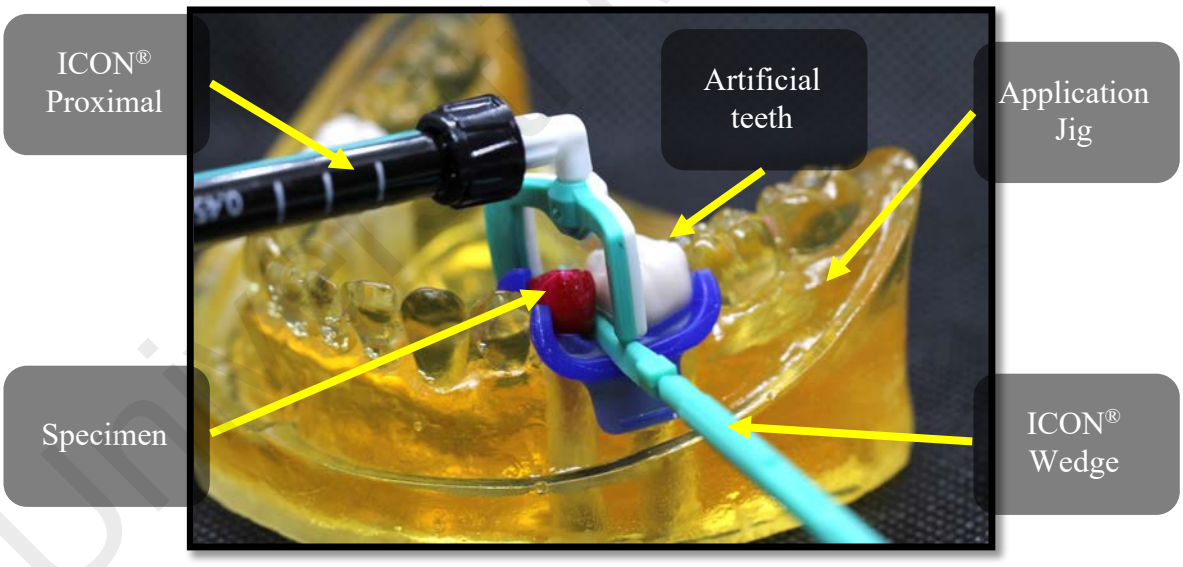

Figure 3.9 Application of ICON® on the proximal surface in the application jig.

Specimens were embedded in epoxy resin (Figure 3.7) prior to surface roughness analysis. Surface roughness measurements using the 3D Alicona were then recorded using standardised scanning and analysing protocols.

Group D

Specimens in group D were treated with fluoride varnish, Duraphat® (Figure 3.10). After initial WSL creation, the specimens were seated into the application jig and the fluoride varnish application protocol will be described in detailed below.

Figure 3.10 Colgate Duraphat® fluoride varnish (22600 ppm fluoride)

The procedure for the varnish application was done in a standard clinical protocol and involved a step-by-step process. The specimens were isolated using a mini dam and wedge to create interproximal space similar to the step that was conducted for the ICON® group. A precision electronic weighing balance (Model: AX224, Sartorius) was used to standardise the amount of varnish (0.2mg) to be applied. A small 0.5mm diameter micro brush was used to place the varnish inside the interproximal space and was evenly spread over the proximal surfaces using a floss (Figure 3.11). Any visible excess varnish was removed using a new floss and a cotton swab pinched by a tweezer. The varnish was left in situ to dry for a further 10 minutes before the surface was washed with running water. The wedge and mini dam were removed.

As with the other groups, specimens were embedded in epoxy resin (Figure 3.7) and surface roughness for each specimen was measured using 3D Alicona.

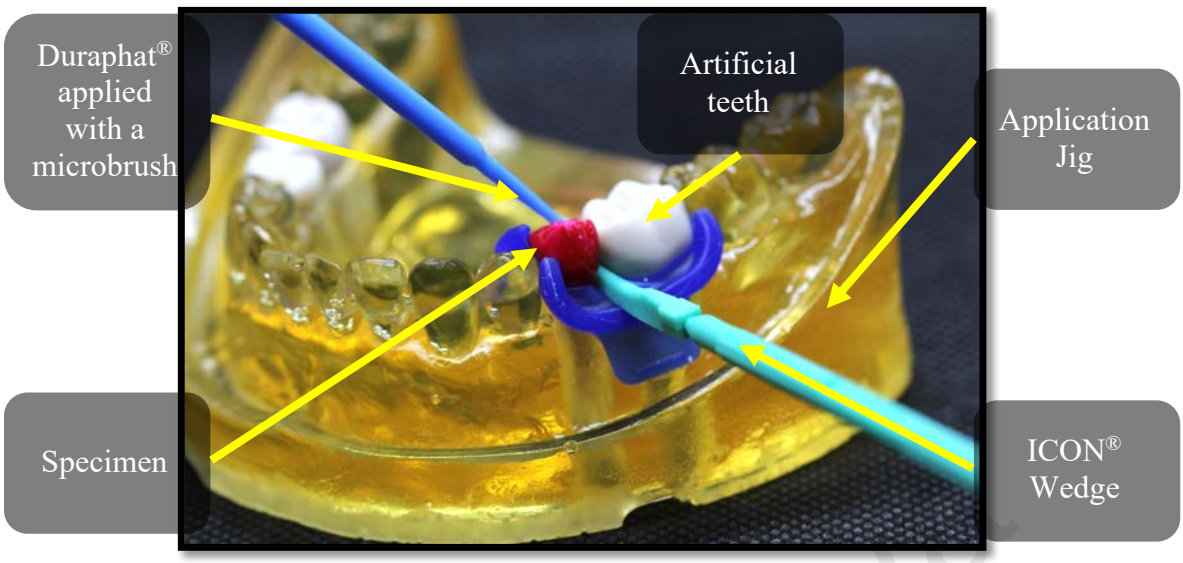

Figure 3.11 Application of Duraphat® on the proximal surface in the application jig

3.2.11 pH Cycling

The demineralisation-remineralisation models used for *in vitro* studies can be divided into biofilm models and chemical models. The biofilm models employ a pure culture system, which used a single strain of bacteria to provide cariogenic challenge. The chemical models can be further divided into simple mineralization models and pH-cycling models (Chu et al., 2012). A modified pH cycling model based on the White & Featherstone model (White et al., 1987) was used for all specimens at 37°C for seven days. Specimens were immersed in a demineralising solution: (2.0 mmol/ L Ca, 2.0 mmol/ L PO_4, 0.075 mol/l acetate buffer, at pH of 4.5) for six hours, alternated with immersion in a remineralising solution: (1.5 mmol/ L Ca, 0.9 mmol/ L PO_4, 0.15 mol/l KCl, 0.02 mol/ L cacodylate buffer, at pH 7.0) for 17 hours for five days (Figure 3.12). The specimens were washed in deionized water for 30 seconds prior to immersion in each solution. The specimens were kept further for two days in a fresh remineralising solution, to complete the 7 days treatment. The specimens were then washed in deionized water for 30 seconds and kept in distilled water prior to surface roughness analysis. Surface

roughness scanning and analysis post pH cycling for all the specimens were again conducted using 3D Alicona using the same standardised settings.

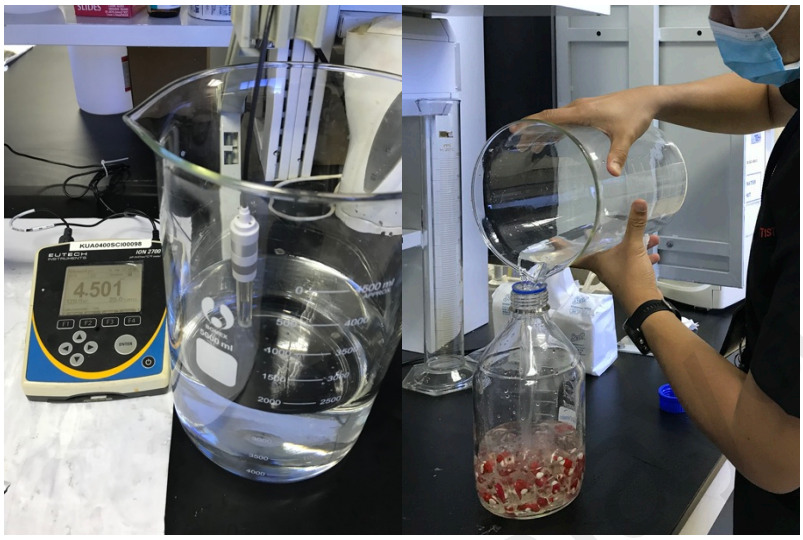

Figure 3.12 Immersion of specimens into demineralising and remineralising solutions (pH cycling)

3.2.12 Measurements of Surface Roughness (Ra)

The measurements using 3D Alicona (Figure 3.13) were performed using the 40X objective at a vertical resolution of 20nm on three areas (each 80×80 µm) on the designated proximal side. 3 profile lines were analysed and the mean surface roughness (R_a) from three readings of each area were recorded for each specimen.

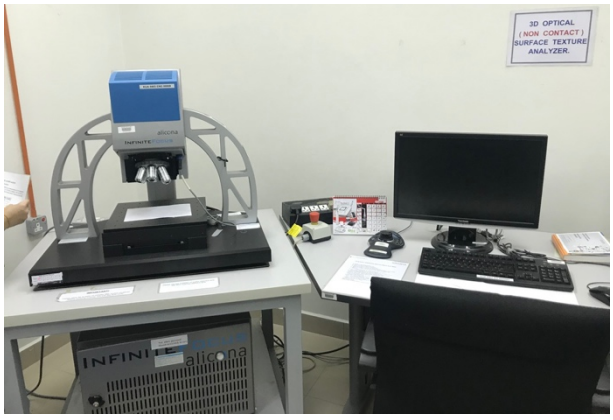

Figure 3.13 The surface profilometer that was used to analyse the surface roughness of the specimens

3D Alicona was also used to capture 3D images of the proximal enamel surfaces (80×80 µm in size) (Figure 3.14).

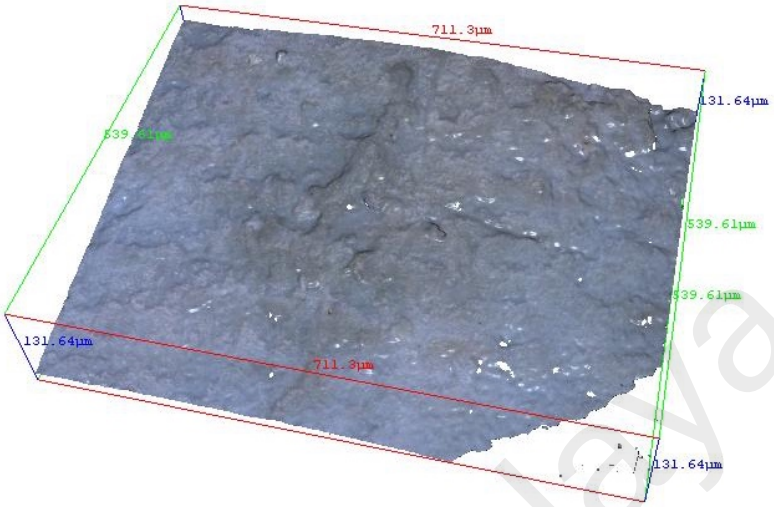

Figure 3.14 Representative 3D topography of the enamel surface using the 3D Alicona

3.2.13 Scanning Electron Microscopy (SEM)

Eight specimens representing each group for each timepoint were separately prepared using the identical step-by-step method and were subjected to SEM analysis. Three images were obtained from each sample at 500x, 2000x and 3000x magnification from the region of interest using the Hitachi VP-SEM SU1510 (Hitachi High Technologies America, Incorporation).

3.2.14 Statistical Analysis

Data collected and descriptive statistics were generated to compare between the groups at each time point. Shapiro-Wilk's tests were then applied to assess assumption of normality. Histogram plots and Shapiro Wilk's test and inspection of skewness were used to determine normality. Before pH cycling, R_a values in all groups except Sound were normally distributed whereas after pH cycling, only R_a values in ICON® and Duraphat® groups were normally distributed.

To compare the mean differences between groups at a single time point, one-way ANOVA and a Dunnet C3 post hoc test was used. Repeated measure ANOVA with Dunnet T3 post hoc test was used to compare the means and the effects of pH cycling on the surface roughness value at before and after pH cycling. Statistical analyses were performed using the SPSS version 23 and the statistical significance level was set at $\alpha = 0.05$

CHAPTER 4: RESULTS

Statistical analysis was conducted using SPSS version 23 (IBM, USA). Histogram plots and Shapiro-Wilk studies were used to determine normality. The assumption of normality as assessed by the Shapiro-Wilk's test ($p > 0.05$) and inspection of skewness revealed the mean surface roughness values (R_a) for all the groups were normally distributed.

4.1 Surface Roughness Comparisons

Surface roughness results (mean, median, standard deviation) for each material at each period of evaluation (before pH cycling, after pH cycling) are shown in Table 4.1. The mean surface roughness (R_a) values for each group before pH cycling recorded were 0.31µm (*SD*=0.03) (Sound), 0.51µm(*SD*=0.04) (Demineralised), 0.31µm (*SD*=0.01) (ICON®), and 0.41µm (*SD*=0.01) (Duraphat®).

The highest R_a value Δ_{before} pH cycling was observed in the Demineralised group (0.51 µm, *SD* = 0.36). Prior to pH cycling, the sound (0.31 µm, *SD* = 0.03) and ICON® (0.31 µm, *SD* = 0.01) demonstrated the lowest R_a values compared to the other groups. The one-way ANOVA test showed that there was a statistically significant difference in R_a between the groups ($P < 0.001$). Post-hoc test showed that there were no statistically significant differences between the sound and ICON® group ($P = 1.000$). All other post-hoc results were statistically significant.

The surface roughness (R_a) values for each group Δ_{after} pH cycling were 0.51µm (*SD*=0.02) (Sound), 0.75µm (*SD*=0.02) (Demineralised), 0.42µm (*SD*=0.01) (ICON®), and 0.58µm (*SD*=0.01) (Duraphat®). The highest Ra value was observed in the Demineralised group (0.75 µm, *SD* = 0.02). After pH cycling, the ICON® (0.42 µm, *SD* = 0.01) group recorded the lowest Ra value when compared to the other groups. The one-

way ANOVA showed that there was a statistically significant difference between the Ra values ($P < 0.001$). In the Dunnet T3 post-hoc results, all the groups showed statistically significant differences ($P < 0.001$). Therefore, we can reject the null hypothesis as the surface roughness were significantly different between ICON® and Duraphat®.

Table 4.1 The surface roughness value (Ra) for each group at each period of evaluation (n=60). (P > 0.05)

Group	Δ_{Before} pH Cycling			Δ_{After} pH Cycling			Mean Difference	**P value
	Mean	SD	Median	Mean	SD	Median		
Sound	0.31	0.03	0.31	0.51	0.02	0.51	0.20	**<0.001**
Demineralised	0.51	0.04	0.51	0.75	0.02	0.75	0.25	**<0.001**
ICON®	0.31	0.01	0.31	0.42	0.01	0.42	0.11	**<0.001**
Duraphat®	0.41	0.01	0.41	0.58	0.01	0.58	0.18	**<0.001**
***P value**	**<0.001**			**<0.001**				

*P values comparing the groups at each time point (one-way ANOVA)
**P values comparing time points for each group (repeated measure ANOVA)

4.2 Surface Roughness Changes

Regarding the comparison of the periods (Δ_{Before}, Δ_{After}) of evaluation for each group, the assumption of sphericity was violated, as assessed by Mauchly's test of sphericity, $\chi2(2) = 0.00$, $p = < 0.05$. Therefore, a Greenhouse-Geisser correction was applied ($\varepsilon = 0.648$). The exercised intervention elicited statistically significant changes in surface roughness of all the materials after pH cycling, $F (1.000, 56.000) = 4679.159$, $p < .001$, partial $\eta2 = 1$. The repeated measure ANOVA test showed statistically significant differences in which there was greater R_a values after pH cycling for all the groups (greater surface roughness at Δ_{After} than at Δ_{Before}).

Results regarding the amount of change in R_a value are shown in Table 4.1. The group with the most changes in R_a value after pH cycling was noted in the Demineralised group, an increase of 0.25 μm from a R_a value of 0.51 μm (*SD*=0.01) to 0.75 μm (*SD*=0.01). The group that was subjected to ICON® infiltration exhibited the least change in R_a value

(0.11 µm) (Figure 4.1). Dunnet T3 post hoc analysis revealed that the mean increase for all the groups were all statistically significant (P = <0.001). Therefore, we can reject the null hypothesis as the result showed significantly different surface roughness after pH cycling in both groups.

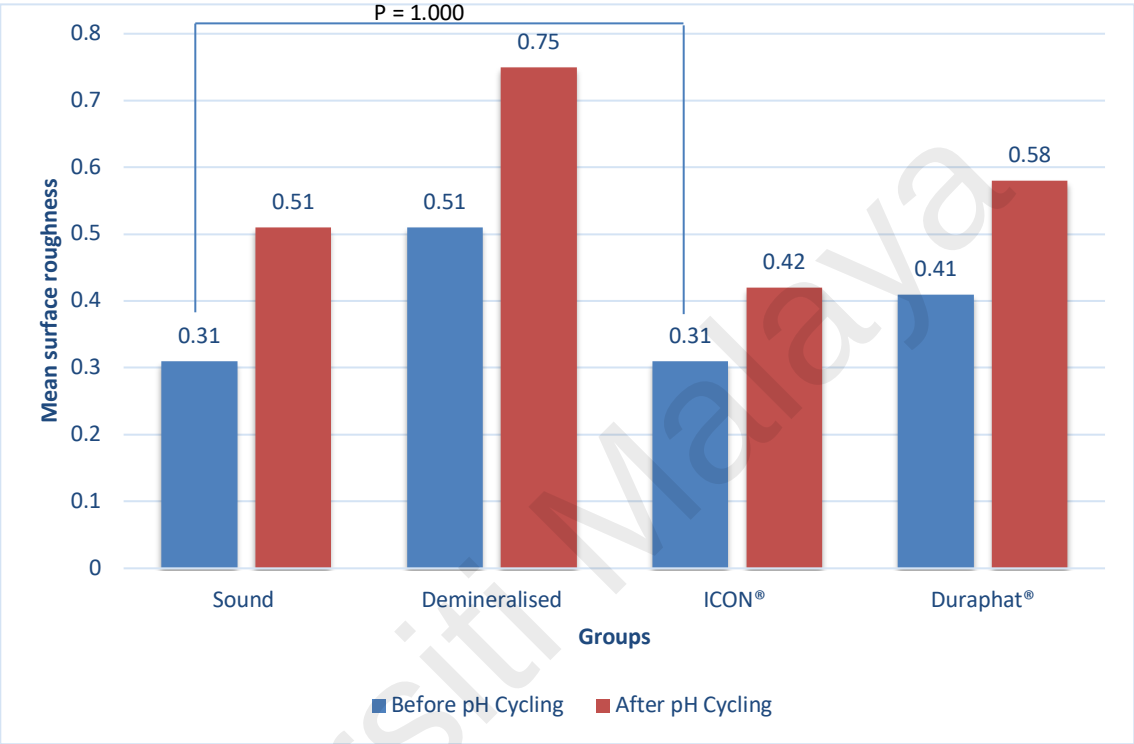

*P (<0.001) comparing the groups at each time point (one-way ANOVA)
**P (<0.001) comparing time points for each group (repeated measure ANOVA)

Figure 4.1 Mean surface roughness for all the groups (µm)

4.3 Surface Topography (Non-Contact Profilometry)

The 3-D interpretation and surface profile for each group at each time point (Δ_{Before} Figure 4.2, Δ_{After} Figure 4.3) was created using the 3D Alicona. All the surfaces showed changes in surface topography with an increase in the depth of pores and valleys after exposure to pH cycling. On the other hand, ICON® group showed minimal changes in surface topography after being subjected to pH cycling for 168 hours compared to the baseline 3-D model (Figure 4.2c, Figure 4.3c).

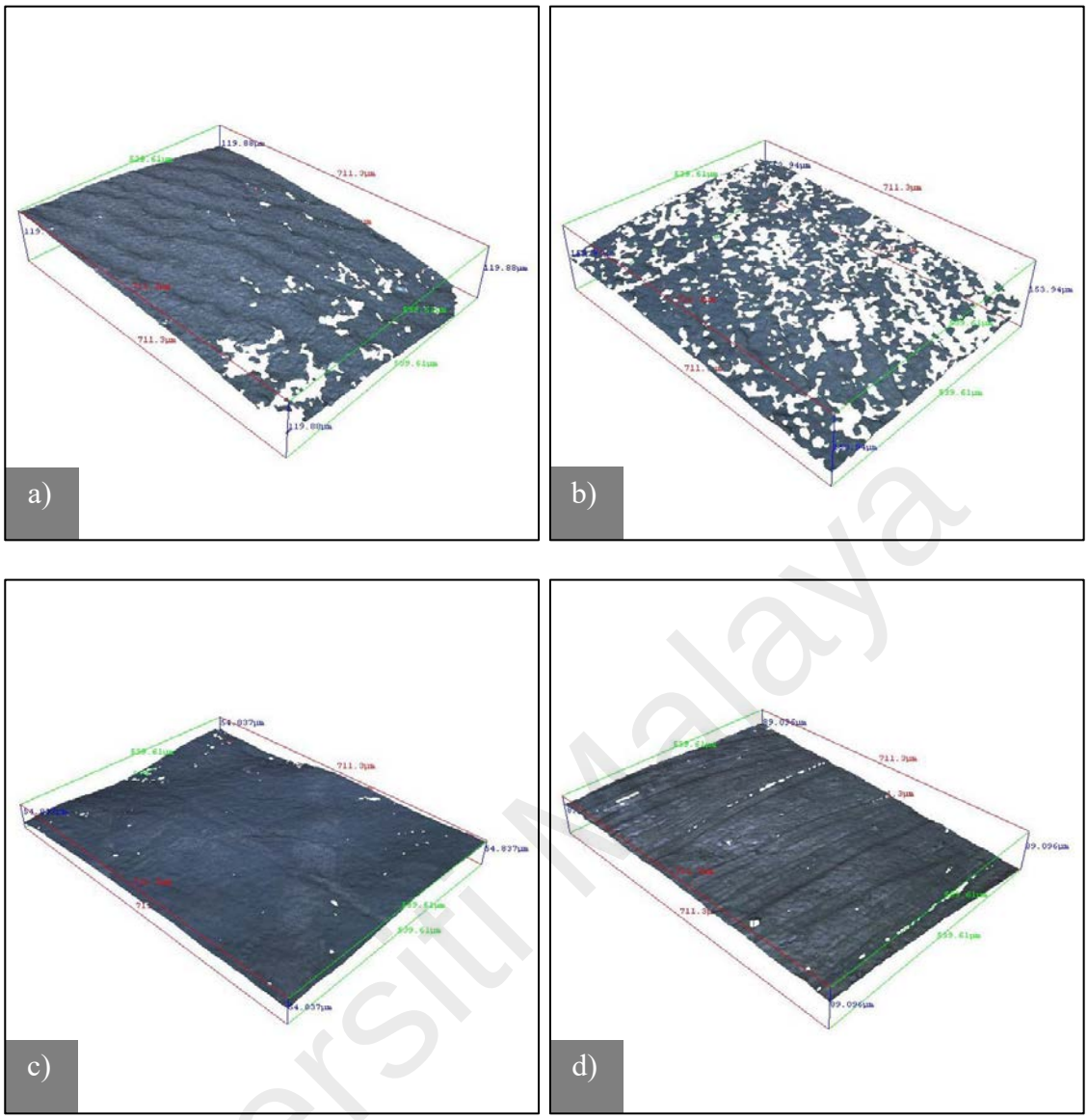

Figure 4.2 The representative 3-Dimensional (3D) interpretation and surface profile of a) Sound b) Demineralised c) ICON® and d) Duraphat® groups before pH cycling.

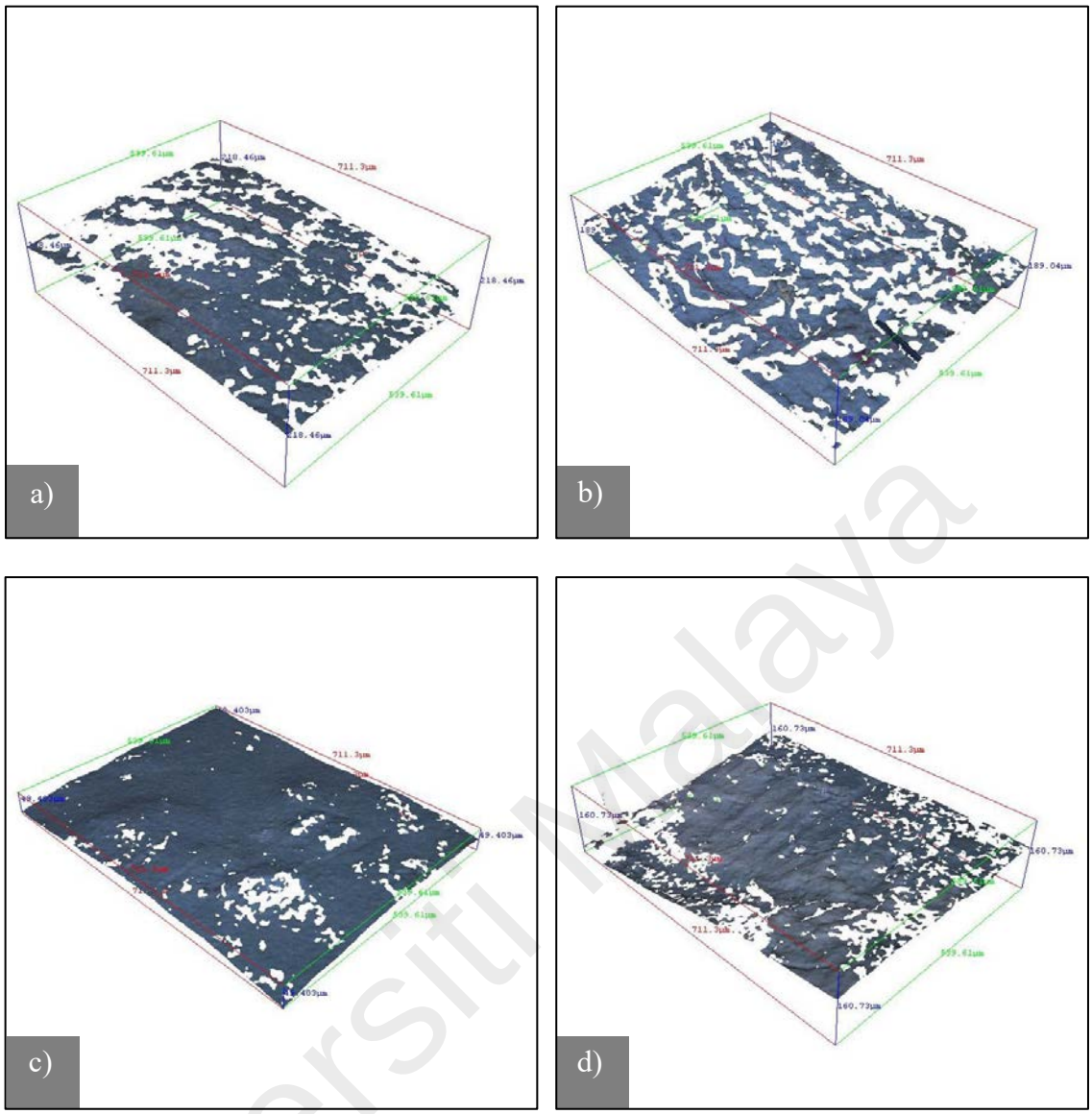

Figure 4.3 The representative 3-Dimensional (3D) interpretation and surface profile of a) Sound b) Demineralised c) ICON® and d) Duraphat® groups after pH cycling.

4.4 Surface Topography (Scanning Electron Microscope)

SEM images of enamel surfaces are shown in Figure 4.4 and Figure 4.5. Figure 4.4a shows the SEM image of a sound tooth obtained at 500x magnification. Figure 4.4b shows the SEM image of a demineralised tooth at equal magnification while Figure 4.4c and Figure 4.4d show images of enamel surfaces treated with ICON® and Duraphat® respectively. Sound enamel (Figure 4.4a) show some pits and scratches, but in general a smooth and nearly homogenous surface. Enamel surface after demineralisation exhibited craters of variable depths which appeared as irregular hexagonal pitted surfaces (Figure

4.4b). The proximal enamel surface treated with ICON® showed blockage of the enamel rods leaving a smooth surface but uneven topography (Figure 4.4c). Surface treated with Duraphat® revealed complete blockage of enamel rods by a continuous mineralised outer layer of fluoride (Figure 4.4d). This mineralised layer appears smooth but with marked vertical lines that coincides with the orientation of flossing.

After pH cycling, evident increase in surface roughness in both Sound (Figure 4.5a) and Demineralised (Figure 4.5b) group, as more hexagonal pitted surface appear as enamel rods loses its core but retains its outer periphery structure. Both the ICON® (Figure 4.5c) and Duraphat® (Figure 4.5d) groups revealed a near-homogenous surface with only slight changes in their morphological features. Both showed localised peeling of the surface revealing honeycomb-shaped enamel rods, in which the prismatic orifices resulting from the pH cycling become more visible. The core of the enamel remains intact.

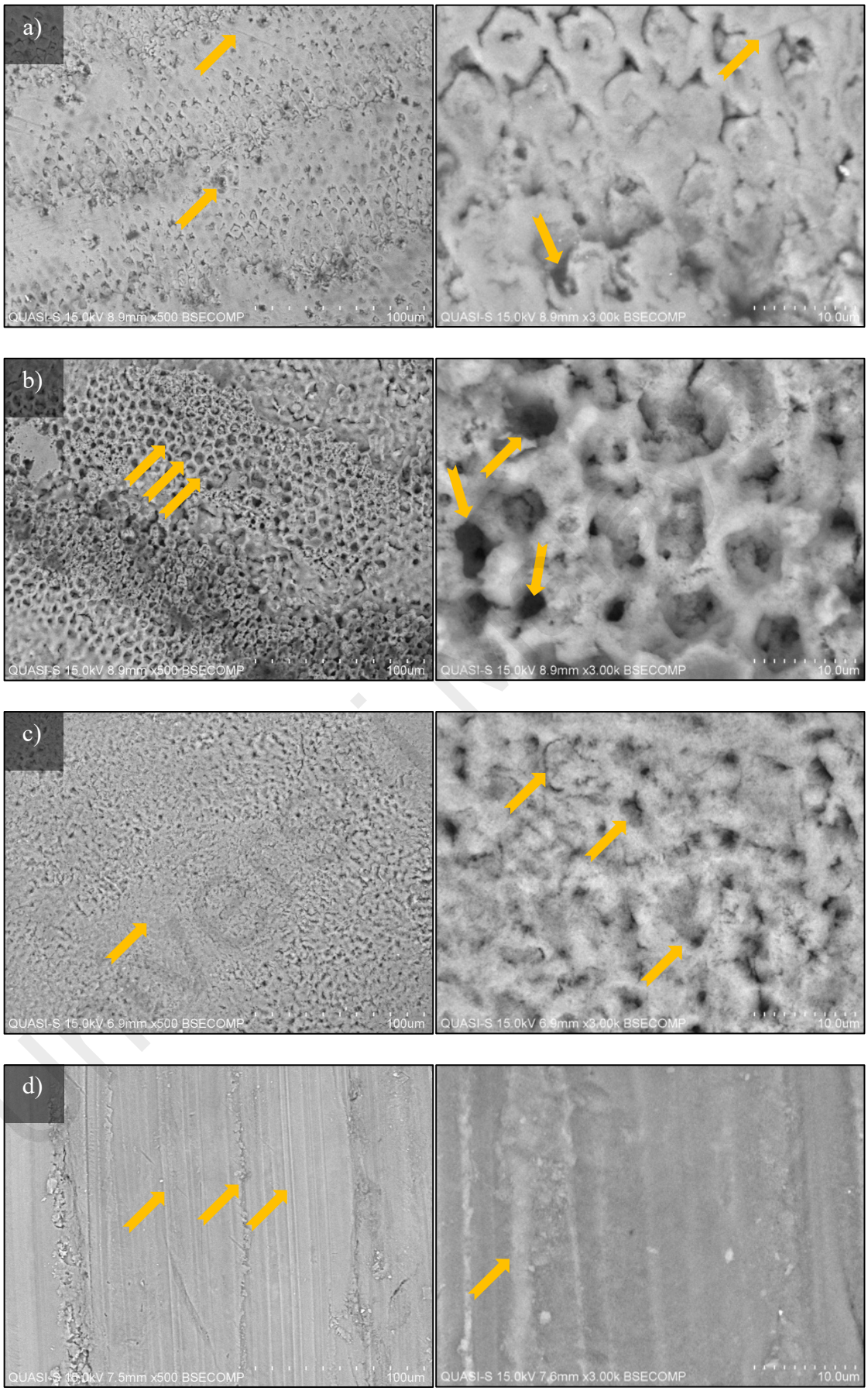

Figure 4.4 (continued) Representative SEM images of enamel surfaces for all the groups (500x, 3000x magnifications): a) Sound; b) Demineralised; c) ICON®; d) Duraphat® before pH cycling (yellow arrows represents surface changes)

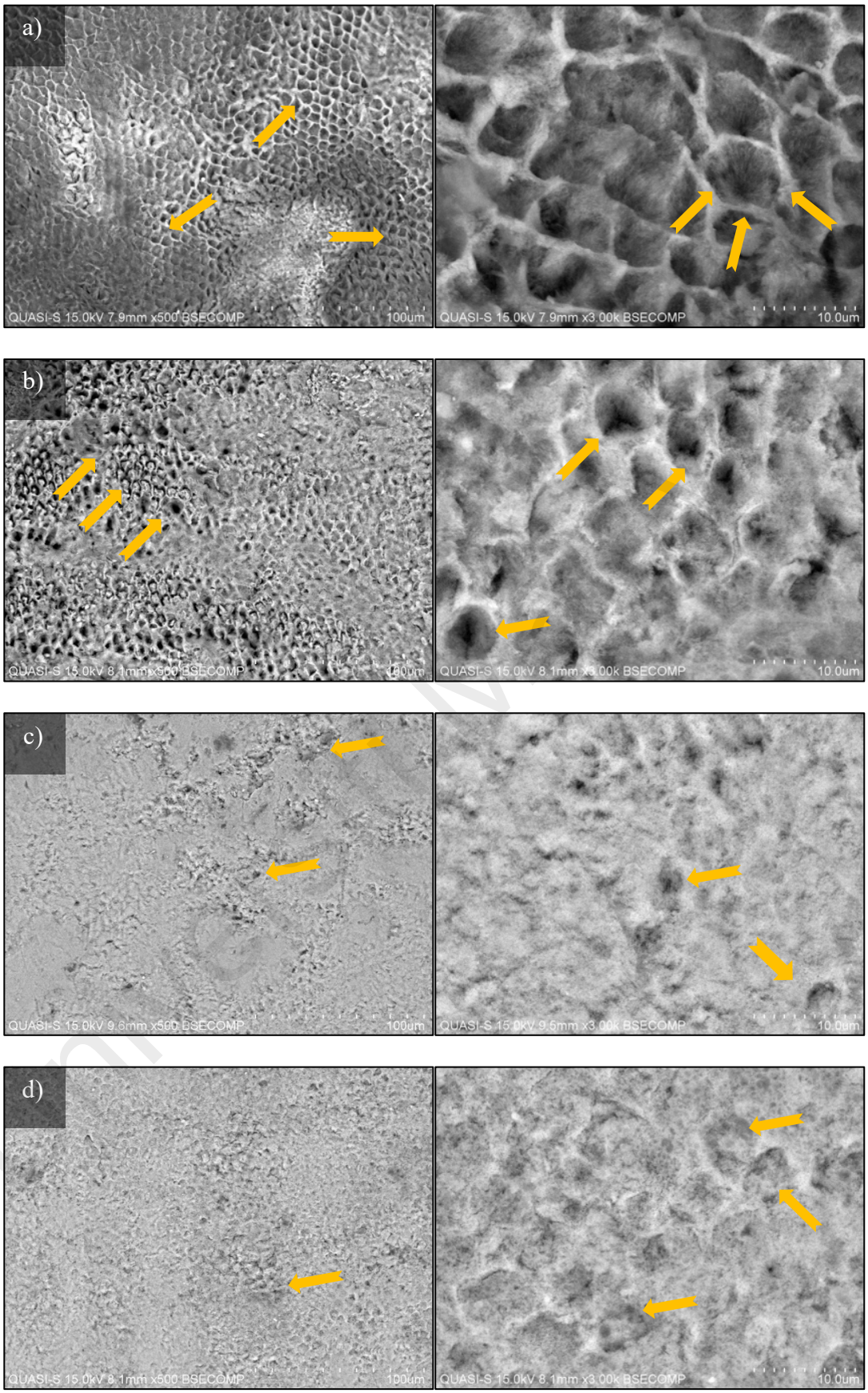

Figure 4.5 Representative SEM images of enamel surfaces for all the groups (500x, 3000x magnifications): a) Sound; b) Demineralised; c) ICON®; d) Duraphat® after pH cycling (yellow arrows represents surface changes)

CHAPTER 5: DISCUSSION

This study aimed to look at the surface roughness of proximal WSLs treated with ICON® and Duraphat® after seven days of acidic challenge. Sample selection and artificially induced WSLs were done via visual inspection and confirmed using optical coherence tomography B-scans.

5.1 Optical Coherence Tomography (OCT)

Early studies on WSLs had been done using conventional methods such as light or stereomicroscopic inspections, polarised light microscopy (Huysmans et al., 2004), confocal microscopy and transverse microradiography (TM) (Meyer-Lueckel et al., 2008; Meyer-Lueckel et al., 2007), scanning electron microscopy (SEM) and atomic force microscope (AFM) (Kielbassa et al., 2006; Taher, 2013). These types of methods have drawbacks where the samples examined are required to be either processed or undergo sectioning which may inevitably alter important structures.

In our study, the idea of analysing the proximal surface and subsurface of WSLs while keeping an intact and clinically relevant enamel surface layer using a non-radiative imaging modality led to the use OCT. What was observed was that WSLs appeared as areas of bright zones in SS-OCT images due to increased backscattering intensity. Previous OCT reports have been focusing on the time-domain PS-OCT systems which has the advantage of decreasing specular reflections from the surface of samples that may interfere with the signal analysis (Baumgartner et al., 2000; Fried et al., 2002; R. S. Jones, Darling, et al., 2006; R. S. Jones & Fried, 2006). On the other hand, findings from this study demonstrated that demineralised enamel can be differentiated sufficiently from sound, healthy enamel using a near infrared based swept-source OCT imaging. Previous studies have reported on significant correlation between SS-OCT and confocal laser scanning microscopy (CLSM) (Figure 5.1) where the actual demineralised area from the

CLSM cross-section corresponded with the bright zone from the SS-OCT B-scan image (Horie et al., 2016; Nakajima et al., 2014; Shimada et al., 2014).

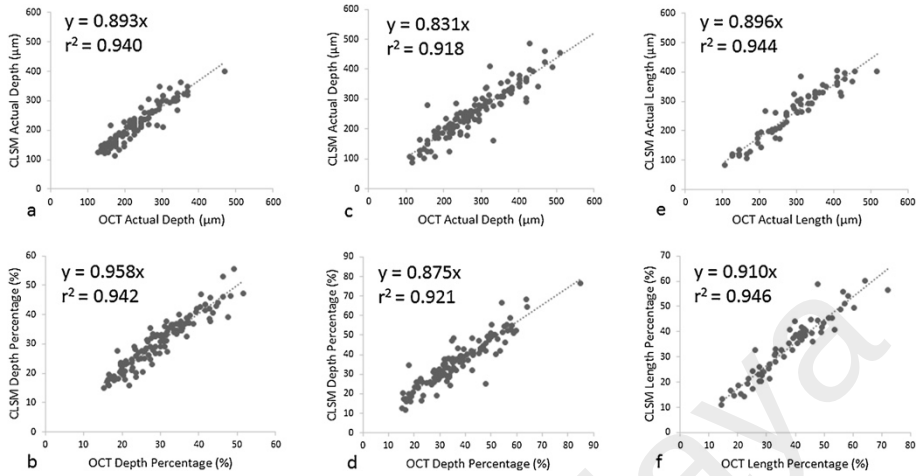

Figure 5.1 Graphs representing relationship between SS-OCT and CLSM measurement with regression with 95% confidence intervals of the linear regression. Significant correlations were observed between SS-OCT and CLSM measurement ($p < 0.001$) (Horie et al., 2016).

Careful considerations were taken when selecting chloramine as the storage medium prior to scanning using the OCT. It has been documented that the use of thymol as a storage medium influences the optical properties of the teeth. Shi et al conducted a study to test the influence of the storage medium on the reading of DIAGNOdnet where they found specimens that were stored in thymol showed a decrease in the fluorescence when compared to teeth stored in formalin (Shi et al., 2001). Chloramine-T solution on the other hand has had no reported effect on optical properties and has been recommended as the infection controlling medium for research purposes involving the enamel surfaces (Humel et al., 2007; Titley et al., 1998; Ziskind et al., 2003).

5.2 Depth of White Spot Lesions (WSLs)

There are two methods of interpreting an OCT data, the first is a quantitative approach that measures back scattering signals intensity and the second is qualitative analysis (B-scans) by investigating the changes in enamel structure in caries and control samples.

It was important to standardise the depth of the artificially induced WSLs to 120–200 μm to eliminate it as a confounding factor. This was based on mean depth of WSLs findings from several authors (V. L. Kumar et al., 2008; Souza Barboza et al., 2019; Ten Cate et al., 1982; Thierens et al., 2019). In our study, SS-OCT qualitative diagnostic capabilities using the B-scans were used to detect changes in the enamel layers. Lesion depth within the range of 120–200 μm in the enamel structure was identified, interpreted, and documented in real-time successfully.

5.3 Experimental Design of the Study

Other *in vitro* demineralisation-remineralisation process in cariology research studies the oral environment and attempts have been made to simulate this environment. The designs vary from simple to complex but even with a complex design it is almost impossible to mimic the complicated process of natural caries development. The detection, diagnosis and treatment of proximal WSLs is difficult because of the restricted direct access to the lesion.

The jig for the current study was created to simulate different clinically relevant situations such as proximal contact points, periodontal ligament simulation and method of delivery of ICON® and Duraphat®. To reduce and possibly eliminate these confounding variables, standardisation using a jig was of importance. According to Gohil et al., proximal contact is not only a point but an area which is usually wider bucco-lingually than occluso-gingivally. The size and firmness of the proximal contacts influences the recurrence of caries around the contact area (Gohil et al., 1973). In the jig, we standardised the specimens' contact area to less than 3mm bucco-lingually and 2mm occluso-gingivally. As proven by Gohil et al, teeth with larger contact dimensions have greater carious incidence. We also took into consideration the importance of a firm

contact area that prevents wedging of food interproximally but also considering the nature of delivering ICON® and Duraphat® that includes interproximal wedging. A separation of around 40-50 μm was needed for successful delivery of both materials (Ntovas et al., 2018; Phark et al., 2009). In order to satisfy both criteria, a polyvinyl siloxane (PVS), which was found to have an elastic modulus similar to human periodontal ligament, was used (Rathi et al., 2018; Soares et al., 2005; Sterzenbach et al., 2011). Specimens were embedded into the jig's simulated socket and the teeth were adjusted to produce interproximal contacts.

The procedure for fluoride application is less technique sensitive when compared to resin infiltration. On the other hand, the post-operative period is more crucial for fluoride as the mechanism of action ranges from 4-6 hours to the next morning. Clinical recommendations by authors on eating and resuming tooth brushing after fluoride varnish application varies from 30 minutes to an hour and 12 hours to 24 hours, respectively (Du et al., 2012). The mean setting time for fluoride varnish is 4 minutes upon contact with saliva (Du et al., 2012; Tewari et al., 1991). In the absence of any saliva containing solutions in our study, we therefore recommended at least 10 minutes of setting time prior to pH cycling.

However, the drawbacks of *in vitro* studies are that the complex structure of the oral cavity, the microbiological effect of oral biofilm, and the hydrodynamic instability of saliva can be hard to imitate. The demineralisation-remineralisation models used for *in vitro* studies can be divided into biofilm models and chemical models. The biofilm models employ a pure culture system, which used a single strain of bacteria to provide cariogenic challenge. The chemical models can be further divided into simple mineralization models and pH-cycling models (Chu et al., 2012).

In our study, we used the pH-cycling model by ten Cate and Duijsters (Ten Cate et al., 1982). This model is based on a scheme to simulate intraoral condition in which a pH neutral environment was periodically interrupted by acid challenges to form a caries lesion. Advantages include the high level of scientific control and the resulting lower variability intrinsic to *in vitro* models, as well as the smaller sample size required (Buzalaf et al., 2010). In the present study, the demineralisation period lasted for 6 hours per day at a pH of 4.5 for 7 days. According to ten Cate and Duijsters (Ten Cate et al., 1982), this demineralisation period simulates a low cariogenic challenge. Argenta et al. (Argenta et al., 2003) reported 60% volume mineral loss from the enamel surface and the lesion depth is similar to that found *in vitro* by Featherstone et al., whose study showed a correlation with clinical data of caries development (Featherstone et al., 1983). Therefore, after one-week of treatment, it was possible to evaluate surface roughness of the enamel.

This fact supports the effectiveness of this modified model in simulating early carious lesions and in studying the initiation and progression of the caries process. It should be emphasized that keeping the specimens in the remineralising solution for additional 2 days after the 5 days of pH-cycling is relevant to preserve the enamel surface layer allowing surface roughness determination.

5.4 Surface Roughness Changes of White Spot Lesions

There are studies that showed changes in the surface roughness after resin infiltration that were not significant (Ulrich et al., 2015) while some have reported that resin infiltrated WSLs exhibited significant rougher enamel surface compared to sound enamel (Kielbassa et al., 2006; Schmidlin et al., 2012). In an experiment using atomic force microscopy showed no significant differences in surface roughness amongst different treatment options, however, these were carried out on sound enamel without any demineralisation (Taher, 2013). In our findings, it may be speculated that degradation of

the resin over a period resulted in a rougher surface. The infiltrant of the resin used in this study was triethylene-glycol-dimethacrylate (TEGDMA) which has been shown to have a relatively high solubility which influences the water absorption and degradation of the polymer (Gajewski et al., 2012).

Surface roughness of the resin influence the adhesion and growth of cariogenic biofilms on their surfaces (Ionescu et al., 2012). From our experiment, the R_a of the untreated initial caries lesion was 0.51µm (*SD*=0.02), which indicated a higher risk for plaque accumulation and further caries progression. The R_a value was 0.31µm (*SD*=0.01) immediately after infiltration. After pH cycling, the R_a value of the ICON® was 0.42µm (*SD*=0.01), which was still above the threshold for plaque retention. All the samples revealed a higher value when compared to the 0.20µm surface roughness threshold value for plaque retention. (Bollenl et al., 1997; Teughels et al., 2006; Ulrich et al., 2015). It is has been reported intraorally patients are able to interpret surface changes when the R_a value is more than 0.50µm (C. S. Jones et al., 2004). Increased surface roughness may result in further plaque accumulation on the surface of the initial caries lesion and promote surface demineralisation and further caries progression.

The results of this study demonstrated that not only infiltrated enamel surface became rougher after pH-cycling, but fluoride varnish also which has been widely used as a caries preventive intervention for more than three decades, showed a similar roughening effect after demineralisation. To our knowledge, the effect of fluoride varnish on surface roughness of enamel has received little, if any, attention. Our findings are best explained by the micromorphological changes that occurs in the enamel due to pH cycling due to increase in porosity and degradation of the enamel and materials (Eskelsen et al., 2018). Yet, the true reason why the surface gets rougher is still open to speculation. These results are also in agreement with results from studies where infiltrated lesions were subjected to

thermocycling in combination with acidic challenges (Kielbassa et al., 2010; Schmidlin et al., 2012; Takashino et al., 2016).

Determination of surface roughness profile along a two-dimensional (2D) line has recently shifted to using areal parameters in three-dimensions. R_a is the two-dimensional (2D) counterpart of the three-dimensional (3D) descriptor S_a. Both reflects the arithmetic mean of the absolute values of the surface point departures from the mean plane of a sampling area but fundamentally different as R_a uses profile filters, and S_a uses an areal filter. The disadvantage of this 2D method is that in repeated measurements, it is almost impossible to replicate the exact same profile line several times. R_a and S_a cannot be compared even if the areal values only differ from profile values by a small margin (Blateyron, 2018). It has shown that on surfaces with regular underlying features R_a approximates S_a well. A tooth has irregular surfaces and materials may appear non-homogenic, thus averaging between 3 to 5 R_a values appears to be a reasonable compromise in time taken and accuracy. An area with more than 10 R_a values showed little to no significance (Lancashire, 2017). The most common form of reporting roughness average within dental studies has been the surface profile (R_a, arithmetic average) (Field et al., 2010). In addition of the need to compare recent areal measurements against literature, which is scarce, on the basis of comparability, R_a was chosen.

In the current study, when we compared sound and treated demineralised enamel, there was a significant increase in the surface roughness in the ICON® group compared to the control group. Although this suggests that the ICON® material has the tendency to increase plaque accumulation in proximal surfaces, there are studies that have in turn shown an increase in surface hardness and caries resistance, thus can be said to perform well clinically in that matter.

In a study done by Taher et al. on human premolars with healthy enamel there was no significant difference in the surface roughness before and after application of ICON® material to enamel using a profilometer (Taher et al., 2012) which is in agreement to our study, albeit a slight increase in the surface roughness of the proximal surface after application of the ICON® using 3D profilometry. In a similar study a year later, Taher reported showing a non–homogenous layer with groups of small enamel grains scattered on the surface when analysed under atomic force microscope (AFM) (Taher, 2013) and this might be the reason for the higher but insignificant increase in surface roughness.

In the present study, the surface roughness results are in agreement with the results of other studies where the ICON® had a significantly rougher surface than the control group (Gurdogan et al., 2017; Ulrich et al., 2015). The difference between Gurdogan's study and our study is their use of sound bovine incisors (smooth buccal surface) in contrast to our study which used human premolars (proximal surface).

This study recorded lower R_a values of fluoride varnish group than the positive control group. Other studies (Ganss et al., 2004; Murakami et al., 2009; Sorvari et al., 1994; Wiegand et al., 2003) have shown that highly concentrated fluoride is able to protect enamel from further demineralisation as calcium fluoride leaches slowly and easily when challenged by acid and prevents the dissolution of minerals from enamel by providing a hyper mineralised physical barrier on the enamel surface (Chow, 1990). These findings and our results are in accordance with other studies (Comar et al., 2015; Levy et al., 2012; Murakami et al., 2009; Sorvari et al., 1994) which found significantly lower values for surface roughness when compared to a group that was not treated with fluoride.

5.5 Relationship Between Surface Roughness and Experimental Design

The cleaning protocols after resin infiltration may have also influenced the differences in the findings due to the difficulty of efficiently removing excess materials from the

proximal surfaces. Paris et al. advised to wipe off the excess infiltrant material before polymerisation because the residual thin resin layer may lead to plaque collection and thus cause decay (Paris et al., 2006). During our experiment, we found that the ICON® material included in the packaging of the ICON® material, involves a syringe from which the substance is dispensed. The quantity of material that is dispensed is much greater than necessary and the excess material must be wiped away with a floss and cotton for the proximal area. No studies simulated the interproximal contacts during application of the materials *in vitro*, thus we believe this contributed to the higher degree of result related to R_a.

There are limitations inherent to the protocols in creating artificial WSLs. The studies included earlier in Chapter 2 differs in the pH of the demineralising agent being used and etching time, and this could be a source of heterogeneity. In a systematic review by Soveral et al, their analysis via meta-regression confirmed that "*pH significantly influences surface roughness in WSLs and resin penetration depth after infiltration technique, and the etching time affected surface roughness and shear bond strength in WSLs*" (Soveral et al., 2021). Their study included an array of studies on both bovine and human teeth that could potentially undermine the consistency of the results, but sensitivity analysis only showed an effect on microhardness in sound enamel specimens, and no significant impact on the remaining parameters. It would be beneficial if future studies be conducted in a harmonised protocol of WSL creation as well the specimen origin towards a more consistent study methodology. In addition, most studies lacked an appropriate rationale for sample size calculation and group allocation of specimens, and these should be accounted for in future studies.

5.6 Limitations of the Study

Laboratory studies similar to our study have some characteristic limitations. They are carried in an artificial and very controlled settings, so it is not possible to generalise the study findings (external validity). The lesions in each tooth may also be different, i.e., the amount of demineralisation in each tooth may vary depending on the amount of fluoride to which they were exposed before extraction. It has been shown that resin infiltration in artificially induced WSLs react differently from a naturally occurring WSLs (Meyer-Lueckel et al., 2007). It is suggestive that the origin of where the samples were collected should be included as an inclusion criteria.

In this *in vitro* study, extracted human maxillary and mandibular premolars were used and the procedure and time needed for the formation of lesions, the application of the treatment material and how the material works on the lesions may be different from what happens *in vivo*. Even with modifications such as applying the materials using a model that mimics intraoral conditions, there will be limitations to some extent. For instance, fluoride varnish hardens upon contact with saliva, thus the absence of saliva might have exaggerated the time spent cleaning the excess materials in our study.

Other limitations in our research are that the laboratory-based research is artificial by kind and pH cycling cannot fully replicate the oral environment. In about one to two weeks of exposure to demineralization acids, the lesions were formed, while oral cavity lesions may develop over a period of months or years.

Our research did not cover the range of possible surface profile orientations. Extensions to the work should consider the effects of sample rotation on the R_a values. A small sample size due to time, unforeseen equipment malfunction, financial constraints and ongoing pandemic are another form of limitation faced while conducting this study.

CHAPTER 6: CONCLUSION

6.1 Conclusion

Within the limitation of this study, it was concluded that:

1. WSLs infiltrated with ICON® exhibited similar surface roughness to sound enamel and remained relatively unchanged after an acidic challenge.
2. Fluoride varnish (Duraphat®) application on proximal white spot lesions increased the surface roughness significantly from sound enamel, but when compared to no intervention, the R_a was significantly lower before and after pH cycling.
3. All the samples revealed a value above the 0.20 µm threshold value for plaque retention.

6.2 Recommendations

Further *in situ* and *in vivo* studies with a larger sample size and other comparable materials are necessary to confirm the results of the present study. A study using the areal filter, S_a and comparing with the current R_a findings may be beneficial in approximating some real-world cases well.

The use of a customised jig to simulate proximal contact can be expanded to compare quality of placement of resin infiltrant to situations where the contact is loose or absent. With this, it is hoped that it will serve as a standard protocol for future studies.

REFERENCES

Abuchaim, C., Rotta, M., Grande, R. H., Loguercio, A. D., & Reis, A. (2010). Effectiveness of sealing active proximal caries lesions with an adhesive system: 1-year clinical evaluation. *Brazilian Oral Research, 24*(3), 361-367.

Adriaenssens, T., & Ughi, G. J. (2017). Recent advances in the field of optical coherence tomography. *Current Cardiovascular Imaging Reports, 10*(7), 1-13.

Akasapu, A., Hegde, U., & Murthy, P. S. (2018). Enamel surface morphology: An ultrastructural comparative study of anterior and posterior permanent teeth. *Journal of Microscopy and Ultrastructure, 6*(3), 160-164.

Almutairi, W. A. (2017). *The association between clinical and radiographic findings in carious primary molar teeth* (Doctoral dissertation,2017). University of Leeds, West Yorkshire, England,

Anderson, P., Beeley, J., Monteiro, P. M., de Soet, H., Andrian, S., Amaechi, B., & Huysmans, M. C. (2011). A European Core Curriculum in Cariology: the knowledge base. *European Journal of Dental Education, 15 Suppl 1*, 18-22.

Ardu, S., Castioni, N. V., Benbachir, N., & Krejci, I. (2007). Minimally invasive treatment of white spot enamel lesions. *Quintessence International, 38*(8), 633-636.

Argenta, R. M., Tabchoury, C. P., & Cury, J. A. (2003). A modified pH-cycling model to evaluate fluoride effect on enamel demineralization. *Pesquisa Odontológica Brasileira, 17*(3), 241-246.

Armstrong, S., Breschi, L., Özcan, M., Pfefferkorn, F., Ferrari, M., & Van Meerbeek, B. (2017). Academy of Dental Materials guidance on in vitro testing of dental composite bonding effectiveness to dentin/enamel using micro-tensile bond strength (μTBS) approach. *Dental Materials, 33*(2), 133-143.

Arnaud, T. M., de Barros Neto, B., & Diniz, F. B. (2010). Chitosan effect on dental enamel de-remineralization: an in vitro evaluation. *Journal of Dentistry, 38*(11), 848-852.

Arslan, S., Zorba, Y. O., Atalay, M. A., Ozcan, S., Demirbuga, S., Pala, K., Ozer, F. (2015). Effect of resin infiltration on enamel surface properties and Streptococcus mutans adhesion to artificial enamel lesions. *Dental Materials, 34*(1), 25-30.

Bader, J. D., Shugars, D. A., Rozier, G., Lohr, K. N., Bonito, A. J., Nelson, J. P., & Jackman, A. M. (2001). Diagnosis and management of dental caries. *Evidence Report Technology Assessment (Summary)*(36), 1-4.

Banting, D., Eggertsson, H., Ekstrand, K., Ferreira-Zandoná, A., Ismail, A., Longbottom, C., Selwitz, R. (2005). Rationale and evidence for the international caries detection and assessment system (ICDAS II). *Ann Arbor, 1001*, 48109-41078.

Barbour, M. E., & Rees, J. S. (2004). The laboratory assessment of enamel erosion: a review. *Journal of Dentistry, 32*(8), 591-602.

Baumgartner, A., Dichtl, S., Hitzenberger, C. K., Sattmann, H., Robl, B., Moritz, A., Sperr, W. (2000). Polarization-sensitive optical coherence tomography of dental structures. *Caries Research, 34*(1), 59-69.

Beauchamp, J., Caufield, P. W., Crall, J. J., Donly, K., Feigal, R., Gooch, B., Simonsen, R. (2008). Evidence-based clinical recommendations for the use of pit-and-fissure sealants: a report of the American Dental Association Council on Scientific Affairs. *The Journal of the American Dental Association, 139*(3), 257-268.

Bergman, G., & Lind, P. O. (1966). A quantitative microradiographic study of incipient enamel caries. *Journal of Dental Research, 45*(5), 1477-1484.

Black, G. (1910). A plea for greater earnestness in the study of caries of the enamel in its relation to the practice of dentistry. *Dentistry Brief, 15*(1), 161.

Blateyron, F. (2018). Does it make sense to compare Ra and Sa values. Retrieved March, 2021, from https://www.digitalsurf.com/blog/does-it-make-sense-to-compare-ra-and-sa-values/.

Bollenl, C. M., Lambrechts, P., & Quirynen, M. (1997). Comparison of surface roughness of oral hard materials to the threshold surface roughness for bacterial plaque retention: a review of the literature. *Dental Materials, 13*(4), 258-269.

Braz, A. K., Aguiar, C. M., & Gomes, A. S. (2011). Evaluation of the integrity of dental sealants by optical coherence tomography. *Dental Materials, 27*(4), e60-64.

Buzalaf, M. A., Hannas, A. R., Magalhaes, A. C., Rios, D., Honorio, H. M., & Delbem, A. C. (2010). pH-cycling models for in vitro evaluation of the efficacy of fluoridated dentifrices for caries control: strengths and limitations. *Journal of Applied Oral Science, 18*(4), 316-334.

Chen, C., Zhang, W., & Liang, Y. (2021). Evaluation of apical root defects during canal instrumentation with two different nickel-titanium (NiTi) systems by optical coherence tomography (OCT) scan. *Journal of Dental Sciences*.

Chow, L. C. (1990). Tooth-bound fluoride and dental caries. *Journal of Dental Research, 69 Spec No*(2_suppl), 595-600; discussion 634-596.

Chu, C. H., Mei, L., Seneviratne, C. J., & Lo, E. C. (2012). Effects of silver diamine fluoride on dentine carious lesions induced by Streptococcus mutans and Actinomyces naeslundii biofilms. *International Journal of Paediatric Dentistry, 22*(1), 2-10.

Colston, B., Sathyam, U., Dasilva, L., Everett, M., Stroeve, P., & Otis, L. (1998). Dental OCT. *Optics Express, 3*(6), 230-238.

Comar, L. P., Cardoso, C. d. A. B., Charone, S., Grizzo, L. T., Buzalaf, M. A. R., & Magalhaes, A. C. (2015). TiF4 and NaF varnishes as anti-erosive agents on

enamel and dentin erosion progression in vitro. *Journal of Applied Oral Science, 23*, 14-18.

Cury, J. A., & Tenuta, L. M. (2009). Enamel remineralization: controlling the caries disease or treating early caries lesions? *Brazilian Oral Research, 23 Suppl 1*, 23-30.

Dawson, A. S., & Makinson, O. F. (1992a). Dental treatment and dental health. Part 1. A review of studies in support of a philosophy of minimum intervention dentistry. *Australian Dental Journal, 37*(2), 126-132.

Dawson, A. S., & Makinson, O. F. (1992b). Dental treatment and dental health. Part 2. An alternative philosophy and some new treatment modalities in operative dentistry. *Australian Dental Journal, 37*(3), 205-210.

De Menezes Oliveira, M. A., Torres, C. P., Gomes-Silva, J. M., Chinelatti, M. A., De Menezes, F. C., Palma-Dibb, R. G., & Borsatto, M. C. (2010). Microstructure and mineral composition of dental enamel of permanent and deciduous teeth. *Microscopy Research and Technique, 73*(5), 572-577.

Deery, C. (2013). Caries detection and diagnosis, sealants and management of the possibly carious fissure. *British Dental Journal, 214*(11), 551-557.

Dirks, O. B. (1961). Longitudinal dental caries study in children 9-15 years of age. *Archives of Oral Biology, 6*, 94-108.

Dorri, M., Dunne, S. M., Walsh, T., & Schwendicke, F. (2015). Micro-invasive interventions for managing proximal dental decay in primary and permanent teeth. *Cochrane Database Systematic Review*(11), CD010431.

Drexler, W., & Fujimoto, J. G. (2008). Optical coherence tomography technology and applications: Springer International Publishing.

Du, M., Cheng, N., Tai, B., Jiang, H., Li, J., & Bian, Z. (2012). Randomized controlled trial on fluoride varnish application for treatment of white spot lesion after fixed orthodontic treatment. *Clinical Oral Investigations, 16*(2), 463-468.

Ekstrand, K. R., Bakhshandeh, A., & Martignon, S. (2010). Treatment of proximal superficial caries lesions on primary molar teeth with resin infiltration and fluoride varnish versus fluoride varnish only: efficacy after 1 year. *Caries Research, 44*(1), 41-46.

El Karim, I. A., Sanhouri, N. M., Hashim, N. T., & Ziada, H. M. (2007). Dental erosion among 12-14 year old school children in Khartoum: a pilot study. *Community Dental Health, 24*(3), 176.

Eskelsen, E., Catelan, A., Hernades, N., Soares, L. E. S., Cavalcanti, A. N., Aguiar, F. H. B., & Liporoni, P. C. S. (2018). Physicochemical changes in enamel submitted to pH cycling and bleaching treatment. *Clinical, Cosmetic and Investigational Dentistry, 10*, 281-286.

Featherstone, J. D. (2008). Dental caries: a dynamic disease process. *Australian Dental Journal, 53*(3), 286-291.

Featherstone, J. D., ten Cate, J. M., Shariati, M., & Arends, J. (1983). Comparison of artificial caries-like lesions by quantitative microradiography and microhardness profiles. *Caries Research, 17*(5), 385-391.

Fejerskov, O., Thylstrup, A., & Larsen, M. J. (1981). Rational use of fluorides in caries prevention: a concept based on possible cariostatic mechanisms. *Acta Odontologica Scandinavica, 39*(4), 241-249.

Feldchtein, F., Gelikonov, V., Iksanov, R., Gelikonov, G., Kuranov, R., Sergeev, A., Warren, J. (1998). In vivo OCT imaging of hard and soft tissue of the oral cavity. *Optics Express, 3*(6), 239-250.

Field, J., Waterhouse, P., & German, M. (2010). Quantifying and qualifying surface changes on dental hard tissues in vitro. *Journal of Dentistry, 38*(3), 182-190.

Frencken, J. E., Peters, M. C., Manton, D. J., Leal, S. C., Gordan, V. V., & Eden, E. (2012). Minimal intervention dentistry for managing dental caries - a review: report of a FDI task group. *International Dental Journal 62*(5), 223-243.

Fried, D., Glena, R. E., Featherstone, J. D., & Seka, W. (1995). Nature of light scattering in dental enamel and dentin at visible and near-infrared wavelengths. *Applied Optics, 34*(7), 1278-1285.

Fried, D., Xie, J., Shafi, S., Featherstone, J. D., Breunig, T. M., & Le, C. (2002). Imaging caries lesions and lesion progression with polarization sensitive optical coherence tomography. *Journal of Biomedical Optics, 7*(4), 618-627.

Gajewski, V. E., Pfeifer, C. S., Fróes-Salgado, N. R., Boaro, L. C., & Braga, R. R. (2012). Monomers used in resin composites: degree of conversion, mechanical properties and water sorption/solubility. *Brazilian Dental Journal, 23*, 508-514.

Ganss, C., Klimek, J., Brune, V., & Schurmann, A. (2004). Effects of two fluoridation measures on erosion progression in human enamel and dentine in situ. *Caries Research, 38*(6), 561-566.

Garcia-Godoy, F., Summitt, J. B., & Donly, K. J. (1997). Caries progression of white spot lesions sealed with an unfilled resin. *Journal of Clinical Pediatric Dentistry, 21*(2), 141-143.

Goepferd, S. J., & Olberding, P. (1989). The effect of sealing white spot lesions on lesion progression in vitro. *Pediatric Dentistry Journal, 11*(1), 14-16.

Gohil, K. S., Talim, S. T., & Singh, I. (1973). Proximal contacts in posterior teeth and factors influencing interproximal caries. *Journal of Prosthetic Dentistry, 30*(3), 295-302.

Gomez, J. (2015). Detection and diagnosis of the early caries lesion. *BMC Oral Health, 15 Suppl 1*(1), S3.

Gray, G. B., & Shellis, P. (2002). Infiltration of resin into white spot caries-like lesions of enamel: an in vitro study. *The European Journal of Prosthodontics and Restorative Dentistry, 10*(1), 27-32.

Groeneveld, A., Van Eck, A., & Dirks, O. B. (1990). Fluoride in caries prevention: is the effect pre-or post-eruptive? *Journal of Dental Research, 69*(2_suppl), 751-755.

Gurdogan, E. B., Ozdemir‐Ozenen, D., & Sandalli, N. (2017). Evaluation of surface roughness characteristics using Atomic Force Microscopy and inspection of microhardness following resin infiltration with ICON®. *Journal of Esthetic and Restorative Dentistry, 29*(3), 201-208.

Hariri, I., Sadr, A., Shimada, Y., Tagami, J., & Sumi, Y. (2012). Effects of structural orientation of enamel and dentine on light attenuation and local refractive index: an optical coherence tomography study. *Journal of Dentistry, 40*(5), 387-396.

Harris, N. O., & Garcia-Godoy, F. (2004). *Primary Preventive Dentistry*: Upper Saddle River, New Jersey: Pearson Education.

Holmgren, C., Gaucher, C., Decerle, N., & Doméjean, S. (2014). Minimal intervention dentistry II: part 3. Management of non-cavitated (initial) occlusal caries lesions–non-invasive approaches through remineralisation and therapeutic sealants. *British Dental Journal, 216*(5), 237-243.

Holtzman, J. S., Osann, K., Pharar, J., Lee, K., Ahn, Y., Tucker, T., Wilder‐Smith, P. (2010). Ability of optical coherence tomography to detect caries beneath commonly used dental sealants. *Lasers in Surgery and Medicine, 42*(8), 752-759.

Horie, K., Shimada, Y., Matin, K., Ikeda, M., Sadr, A., Sumi, Y., & Tagami, J. (2016). Monitoring of cariogenic demineralization at the enamel–composite interface using swept-source optical coherence tomography. *Dental Materials, 32*(9), 1103-1112.

Horner, K., & Eaton, K. (2018). Selection criteria for dental radiography - Third Edition. Retrieved March 10, 2021, from https://cgdent.uk/wp-content/uploads/2021/08/FGDP-SCDR-ALL-Web.pdf

Hsieh, Y. S., Ho, Y. C., Lee, S. Y., Chuang, C. C., Tsai, J. C., Lin, K. F., & Sun, C. W. (2013). Dental optical coherence tomography. *Sensors (Basel), 13*(7), 8928-8949.

Humel, M. M. C., Oliveira, M. T., Cavalli, V., & Giannini, M. (2007). Effect of storage and disinfection methods of extracted bovine teeth on bond strength to dentin. *Brazilian Journal of Oral Sciences*.

Huysmans, M. C., & Longbottom, C. (2004). The challenges of validating diagnostic methods and selecting appropriate gold standards. *Journal of Dental Research, 83*, 48-52.

Innes, N. P., Frencken, J. E., Bjorndal, L., Maltz, M., Manton, D. J., Ricketts, D., Schwendicke, F. (2016). Managing carious lesions: Consensus recommendations on terminology. *Advances in Dental Research, 28*(2), 49-57.

Ionescu, A., Wutscher, E., Brambilla, E. o., Schneider‐Feyrer, S., Giessibl, F. J., & Hahnel, S. (2012). Influence of surface properties of resin‐based composites on in vitro S treptococcus mutans biofilm development. *European Journal of Oral Sciences, 120*(5), 458-465.

Ishibashi, K., Ozawa, N., Tagami, J., & Sumi, Y. (2011). Swept-source optical coherence tomography as a new tool to evaluate defects of resin-based composite restorations. *Journal of Dentistry, 39*(8), 543-548.

Jang, I. (2020). *Cardiovascular OCT Imaging*. Cham, Switzerland: Springer.

Jones, C. S., Billington, R. W., & Pearson, G. J. (2004). The in vivo perception of roughness of restorations. *British Dental Journal, 196*(1), 42-45.

Jones, R. S., Darling, C. L., Featherstone, J. D., & Fried, D. (2006). Imaging artificial caries on the occlusal surfaces with polarization-sensitive optical coherence tomography. *Caries Research, 40*(2), 81-89.

Jones, R. S., & Fried, D. (2006). Remineralization of enamel caries can decrease optical reflectivity. *Journal of Dental Research, 85*(9), 804-808.

Kaitsas, V., & Olivi, G. (2015). Structure and ultrastructure of the hard tissue of the human teeth. In *Lasers in Restorative Dentistry* (3-22): Springer, Berlin, Heidelberg.

Karlsson, L. (2010). Caries detection methods based on changes in optical properties between healthy and carious tissue. *International Journal of Dentistry, 2010*.

Kidd, E. A., & Fejerskov, O. (2016). *Essentials of Dental Caries*: Oxford University Press.

Kielbassa, A. M., Paris, S., Lussi, A., & Meyer-Lueckel, H. (2006). Evaluation of cavitations in proximal caries lesions at various magnification levels in vitro. *Journal of Dentistry, 34*(10), 817-822.

Kielbassa, A. M., Ulrich, I., Treven, L., & Mueller, J. (2010). An updated review on the resin infiltration technique of incipient proximal enamel lesions. *Medicine Evolution, 16*(4), 3-15.

Kielbassa, A. M., Wrbas, K. T., Schulte-Monting, J., & Hellwig, E. (1999). Correlation of transversal microradiography and microhardness on in situ-induced demineralization in irradiated and nonirradiated human dental enamel. *Archives of Oral Biology, 44*(3), 243-251.

Kim, S., Kim, E. Y., Jeong, T. S., & Kim, J. W. (2011). The evaluation of resin infiltration for masking labial enamel white spot lesions. *International Journal ofPpaediatric Dentistry, 21*(4), 241-248.

Kumar, G. S. (2015). *Orban's Oral Histology and Embryology*: Elsevier India.

Kumar, V. L., Itthagarun, A., & King, N. M. (2008). The effect of casein phosphopeptide-amorphous calcium phosphate on remineralization of artificial caries-like lesions: an in vitro study. *Australian Dental Journal, 53*(1), 34-40.

Lakshmikantha, H. T., Ravichandran, N. K., & Park, H.-S. (2017). Current trends and clinical applications of optical coherence tomography in orthodontics: a literature review. *Dental and Medical Problems, 54*(4), 409-415.

Lancashire, H. T. (2017). A simulated comparison between profile and areal surface parameters: Ra as an estimate of Sa. Retrieved March 11, 2021, from https://arxiv.org/abs/1708.02284.

Larsen, M. J., & Fejerskov, O. (1987). Remineralization from a clinical point of view. *Deutsche Zahnarztliche Zeitschrift, 42*(10 Suppl 1), 91-94.

Larsen, M. J., & Fejerskov, O. (1989). Chemical and structural challenges in remineralization of dental enamel lesions. *Scandinavian Journal of Dental Research, 97*(4), 285-296.

Leroy, N., & Bres, E. (2001). Structure and substitutions in fluorapatite. *European Cells & Materials, 2*, 36-48.

Levy, F. M., Magalhaes, A. C., Gomes, M. F., Comar, L. P., Rios, D., & Buzalaf, M. A. R. (2012). The erosion and abrasion‐inhibiting effect of TiF4 and NaF varnishes and solutions on enamel in vitro. *International Journal of Paediatric Dentistry, 22*(1), 11-16.

Lussi, A. (2006). *Dental erosion: from diagnosis to therapy* (Vol. 20): Karger Medical and Scientific Publishers.

Machale, P. S., Hegde-Shetiya, S., & Agarwal, D. (2013). The incipient caries. *Journal of Contemporary Dentistry, 3*(1), 20-24.

Machoy, M., Seeliger, J., Szyszka-Sommerfeld, L., Koprowski, R., Gedrange, T., & Woźniak, K. (2017). The use of optical coherence tomography in dental diagnostics: a state-of-the-art review. *Journal of Healthcare Engineering, 2017*.

Mann, A., & Dickinson, M. (2006). Nanomechanics, chemistry and structure at the enamel surface. *Monographs in oral science, 19*, 105.

Martignon, S., Ekstrand, K. R., & Ellwood, R. (2006). Efficacy of sealing proximal early active lesions: an 18-month clinical study evaluated by conventional and subtraction radiography. *Caries Research, 40*(5), 382-388.

Martignon, S., Ekstrand, K. R., Gomez, J., Lara, J. S., & Cortes, A. (2012). Infiltrating/sealing proximal caries lesions: a 3-year randomized clinical trial. *Journal of Dental Research, 91*(3), 288-292.

Mertz-Fairhurst, E. J., Curtis Jr, J. W., Ergle, J. W., Rueggeberg, F. A., & Adair, S. M. (1998). Ultraconservative and cariostatic sealed restorations: results at year 10. *The Journal of the American Dental Association, 129*(1), 55-66.

Meyer-Lueckel, H., & Paris, S. (2008). Improved resin infiltration of natural caries lesions. *Journal of Dental Research, 87*(12), 1112-1116.

Meyer-Lueckel, H., Paris, S., & Kielbassa, A. M. (2007). Surface layer erosion of natural caries lesions with phosphoric and hydrochloric acid gels in preparation for resin infiltration. *Caries Research, 41*(3), 223-230.

Mount, G. J. (1991). Minimal treatment of the carious lesion. *International Dental Journal, 41*(1), 55-59.

Murakami, C., Bonecker, M., Correa, M. S., Mendes, F. M., & Rodrigues, C. R. (2009). Effect of fluoride varnish and gel on dental erosion in primary and permanent teeth. *Archives of Oral Biology, 54*(11), 997-1001.

Nakajima, Y., Shimada, Y., Sadr, A., Wada, I., Miyashin, M., Takagi, Y., Sumi, Y. (2014). Detection of occlusal caries in primary teeth using swept source optical coherence tomography. *Journal of Biomedical Optics, 19*(1), 016020.

Ntovas, P., & Rahiotis, C. (2018). A clinical guideline for caries infiltration of proximal enamel lesions with resins. *British Dental Journal, 225*(4), 299-304.

Nyvad, B., & Fejerskov, O. (1997). Assessing the stage of caries lesion activity on the basis of clinical and microbiological examination. *Community Dentistry and Oral Epidemiology, 25*(1), 69-75.

Otis, L. L., Everett, M. J., Sathyam, U. S., & Colston, B. W., Jr. (2000). Optical coherence tomography: a new imaging technology for dentistry. *The Journal of the American Dental Association, 131*(4), 511-514.

Paris, S., Hopfenmuller, W., & Meyer-Lueckel, H. (2010). Resin infiltration of caries lesions: an efficacy randomized trial. *Journal of Dental Research, 89*(8), 823-826.

Paris, S., & Meyer-Lueckel, H. (2009). Masking of labial enamel white spot lesions by resin infiltration-a clinical report. *Quintessence International, 40*(9).

Paris, S., & Meyer-Lueckel, H. (2010). Infiltrants inhibit progression of natural caries lesions in vitro. *Journal of Dental Research, 89*(11), 1276-1280.

Paris, S., Meyer-Lueckel, H., Mueller, J., Hummel, M., & Kielbassa, A. M. (2006). Progression of sealed initial bovine enamel lesions under demineralizing conditions in vitro. *Caries Research, 40*(2), 124-129.

Park, S.-E., Yi, K., Kim, H.-Y., Son, H.-H., & Chang, J. (2011). Elemental analysis of the fluoride varnish effects on root caries initiation. *Journal of Korean Academy of Conservative Dentistry, 36*(4), 290-299.

Peters, M. C., & McLean, M. E. (2001). Minimally invasive operative care. I. Minimal intervention and concepts for minimally invasive cavity preparations. *The Journal of Adhesive Dentistry, 3*(1), 7-16.

Phark, J. H., Duarte, S., Jr., Meyer-Lueckel, H., & Paris, S. (2009). Caries infiltration with resins: a novel treatment option for interproximal caries. *Compendium of Continuing Education in Dentistry, 30 Spec No 3*, 13-17.

Potsaid, B., Baumann, B., Huang, D., Barry, S., Cable, A. E., Schuman, J. S., Fujimoto, J. G. (2010). Ultrahigh speed 1050nm swept source/Fourier domain OCT retinal and anterior segment imaging at 100,000 to 400,000 axial scans per second. *Optics Express, 18*(19),29-48.

Rathi, A., Chowdhry, P., Kaushik, M., Reddy, P., Roshni, & Mehra, N. (2018). Effect of different periodontal ligament simulating materials on the incidence of dentinal cracks during root canal preparation. *Journal of Dental Research, Dental Clinics, Dental Prospects, 12*(3), 196-200.

Roberson, T., Heymann, H., & Swift, E. J. & Sturdevant C. M. (2006). *Sturdevant's art and science of operative dentistry*: Elsevier Health Sciences., Orlando.

Robinson, C., Brookes, S., Kirkham, J., Wood, S., & Shore, R. (2001). In vitro studies of the penetration of adhesive resins into artificial caries–like lesions. *Caries Research, 35*(2), 136-141.

Robinson, C., Hallsworth, A. S., Weatherell, J. A., & Kunzel, W. (1976). Arrest and control of carious lesions: a study based on preliminary experiments with resorcinol-formaldehyde resin. *Journal of Dental Research, 55*(5), 812-818.

Rodda, J. C. (1983). Impregnation of caries-like lesions with dental resins. *New Zealand Dental Journal, 79*(358), 114-117.

Rodriguez, J. M., Curtis, R. V., & Bartlett, D. W. (2009). Surface roughness of impression materials and dental stones scanned by non-contacting laser profilometry. *Dental Materials Journal, 25*(4), 500-505.

Rølla, G., Øsard, B., & de Almeida Cruz, R. (1993). Topical application of fluorides on teeth: new concepts of mechanisms of interaction. *Journal of Clinical Periodontology, 20*(2), 105-108.

Santamaria, R. M., Innes, N. P., Machiulskiene, V., Evans, D. J., Alkilzy, M., & Splieth, C. H. (2015). Acceptability of different caries management methods for primary molars in a RCT. *International Journal of Paediatric Dentistry, 25*(1), 9-17.

Schlüter, N., Hara, A., Shellis, R., & Ganss, C. (2011). Methods for the measurement and characterization of erosion in enamel and dentine. *Caries Research, 45*(1), 13-23.

Schmidlin, P. R., Sener, B., Attin, T., & Wiegand, A. (2012). Protection of sound enamel and artificial enamel lesions against demineralisation: caries infiltrant versus adhesive. *Journal of Dentistry, 40*(10), 851-856.

Schmidt-Nielsen, B. (1946). The solubility of tooth substance in relation to the composition of saliva. *Acta Odontologica Scandinavica, 7*(2), 1-86.

Senawongse, P., Pongprueksa, P., Harnirattisai, C., Sumi, Y., Otsuki, M., Shimada, Y., & Tagami, J. (2011). Non-destructive assessment of cavity wall adaptation of

class V composite restoration using swept-source optical coherence tomography. *Dental Materials Journal*, 2011; 30(4): 517–522.

Shemesh, H., van Soest, G., Wu, M. K., van der Sluis, L. W., & Wesselink, P. R. (2007). The ability of optical coherence tomography to characterize the root canal walls. *Journal of Endodontics, 33*(11), 1369-1373.

Shi, X. Q., Tranaeus, S., & Angmar-Mansson, B. (2001). Validation of DIAGNOdent for quantification of smooth-surface caries: an in vitro study. *Acta Odontologica Scandinavica, 59*(2), 74-78.

Shimada, Y., Nakagawa, H., Sadr, A., Wada, I., Nakajima, M., Nikaido, T., Sumi, Y. (2014). Noninvasive cross‐sectional imaging of proximal caries using swept‐source optical coherence tomography (SS‐OCT) in vivo. *Journal of Biophotonics, 7*(7), 506-513.

Silverstone, L. (1982). Relationship of the macroscopic, histological and radiographic appearance of interproximal lesions in human teeth: in vitro study using artificial caries technique. *Pediatric Dentistry Journal, 3*(suppl 2), 414-422.

Soares, C. J., Pizi, E. C. G., Fonseca, R. B., & Martins, L. R. M. (2005). Influence of root embedment material and periodontal ligament simulation on fracture resistance tests. *Brazilian Oral Research, 19*, 11-16.

Sorvari, R., Meurman, J. H., Alakuijala, P., & Frank, R. M. (1994). Effect of fluoride varnish and solution on enamel erosion in vitro. *Caries Research, 28*(4), 227-232.

Souza Barboza, A. C., Fraga Briso, A. L., Moda, M. D., Gallinari, M. D. O., Bresciani, E., Dos Santos, P. H., & Fagundes, T. C. (2019). Colour change and surface gloss of unpolished infiltrated bovine enamel submitted to toothbrushing, pH cycling and artificial ageing. *Journal Of Clinical And Diagnostic Research*, 23-26.

Soveral, M., Machado, V., Botelho, J., Mendes, J. J., & Manso, C. (2021). Effect of resin infiltration on enamel: A systematic review and meta-analysis. *Journal of Functional Biomaterial, 12*(3), 48.

Sterzenbach, G., Kalberlah, S., Beuer, F., Frankenberger, R., & Naumann, M. (2011). In-vitro simulation of tooth mobility for static and dynamic load tests: a pilot study. *Acta Odontologica Scandinavica, 69*(5), 316-318.

Subramaniam, P., Babu, K. G., & Lakhotia, D. (2014). Evaluation of penetration depth of a commercially available resin infiltrate into artificially created enamel lesions: An in vitro study. *Journal of Conservative Dentistry, 17*(2), 146.

Taher, N. M. (2013). Atomic force microscopy and tridimensional topography analysis of human enamel after resinous infiltration and storage in water. *Saudi Medical Journal, 34*(4), 408-414.

Taher, N. M., Alkhamis, H. A., & Dowaidi, S. M. (2012). The influence of resin infiltration system on enamel microhardness and surface roughness: An in vitro study. *Saudi Dental Journal, 24*(2), 79-84.

Takashino, N., Nakashima, S., Shimada, Y., Tagami, J., & Sumi, Y. (2016). Effect of thermal cyclic stress on acid resistance of resin-infiltrated incipient enamel lesions in vitro. *Dental Materials Journal, 35*(3), 425-431.

Ten Bosch, J., & Angmar-Månsson, B. (1991). Invited review: A review of quantitative methods for studies of mineral content of intra-oral incipient caries lesions. *Journal of Dental Research, 70*(1), 2-14.

Ten Cate, J. M. (2003). Chemical interactions between the tooth and oral fluids. *Dental caries: the disease and its clinical management*. (49-69). Blackwell Publishing. Oxford.

Ten Cate, J. M., & Duijsters, P. P. (1982). Alternating demineralization and remineralization of artificial enamel lesions. *Caries Research, 16*(3), 201-210.

Ten Cate, J. M., Timmer, K., Shariati, M., & Featherstone, J. D. (1988). Effect of timing of fluoride treatment on enamel de- and remineralization in vitro: a pH-cycling study. *Caries Research, 22*(1), 20-26.

Teughels, W., Van Assche, N., Sliepen, I., & Quirynen, M. (2006). Effect of material characteristics and/or surface topography on biofilm development. *Clinical Oral Implants Research, 17*(S2), 68-81.

Tewari, A., Chawla, H., & Utreja, A. (1991). Comparative evaluation of the role of NaF, APF & Duraphat topical fluoride applications in the prevention of dental caries--a 2 1/2 years study. *Journal of the Indian Society of Pedodontics and Preventive Dentistry, 8*(1), 28-35.

Thierens, L. A. M., Moerman, S., Elst, C. V., Vercruysse, C., Maes, P., Temmerman, L., Pauw, G. A. M. (2019). The in vitro remineralizing effect of CPP-ACP and CPP-ACPF after 6 and 12 weeks on initial caries lesion. *Journal of Applied Oral Science, 27*.

Titley, K., Chernecky, R., Rossouw, P., & Kulkarni, G. (1998). The effect of various storage methods and media on shear-bond strengths of dental composite resin to bovine dentine. *Archives of Oral Biology, 43*(4), 305-311.

Tyas, M. J., Anusavice, K. J., Frencken, J. E., & Mount, G. J. (2000). Minimal intervention dentistry--a review. FDI Commission Project 1-97. *International Dental Journal, 50*(1), 1-12.

Ulrich, I., Mueller, J., Wolgin, M., Frank, W., & Kielbassa, A. M. (2015). Tridimensional surface roughness analysis after resin infiltration of (deproteinized) natural subsurface carious lesions. *Clinical Oral Investigations, 19*(6), 1473-1483.

Uribe, S. (2006). Summary guideline. Prevention and management of dental decay in the pre-school child. *Evidence-based Dentistry, 7*(1), 4-7.

Warreth, A., Abuhijleh, E., Almaghribi, M. A., Mahwal, G., & Ashawish, A. (2020). Tooth surface loss: A review of literature. *Saudi Dental Journal, 32*(2), 53-60.

Waterhouse, P. J., Auad, S. M., Nunn, J. H., Steen, I. N., & Moynihan, P. J. (2008). Diet and dental erosion in young people in south-east Brazil. *International Journal of Paediatric Pentistry, 18*(5), 353-360.

White, D. J., & Featherstone, J. D. (1987). A longitudinal microhardness analysis of fluoride dentifrice effects on lesion progression in vitro. *Caries Research, 21*(6), 502-512.

Wiegand, A., & Attin, T. (2003). Influence of fluoride on the prevention of erosive lesions - a review. *Oral Health and Preventive Dentistry, 1*(4), 245-253.

Wilder-Smith, P., Otis, L., Zhang, J., & Chen, Z. (2008). Dental OCT. In *Optical Coherence Tomography* (pp. 1151-1182): Springer, Cham, Switzerland.

Yun, S., Tearney, G., Bouma, B., Park, B., & de Boer, J. F. (2003). High-speed spectral-domain optical coherence tomography at 1.3 μm wavelength. *Optics Express, 11*(26), 3598-3604.

Ziskind, D., Gleitman, J., Rotstein, I., & Friedman, M. (2003). Evaluation of cetylpyridinium chloride for infection control in storage solution. *Journal of Oral Rehabilitation, 30*(5), 477-481.

LIST OF PUBLICATIONS AND PAPERS PRESENTED

1. Oral presentation at the 20th Annual Scientific Meeting of International Association for Dental Research IADR Malaysian Section
2. Oral presentation at the 14th Dental Postgraduate Conference 2021, Faculty of Dentistry, University of Malaya